Korean Journal of Radiology

KJR

Non-Infectious Granulomatous Lung Disease: Imaging Findings with Pathologic Correlation

Tomás Franquet[1], Teri J. Franks[2], Jeffrey R. Galvin[3], Edson Marchiori[4], Ana Giménez[1], Sandra Mazzini[1], Takeshi Johkoh[5], Kyung Soo Lee[6]

[1]Department of Diagnostic Radiology, Hospital de Sant Pau, Universitat Autónoma de Barcelona, Barcelona, Spain; [2]Department of Defense, Pulmonary & Mediastinal Pathology, The Joint Pathology Center, Silver Spring, MD, USA; [3]Department of Diagnostic Radiology, Chest Imaging, & Pulmonary Critical Care Medicine, University of Maryland School of Medicine, Baltimore, MD, USA; [4]Department of Radiology, Hospital Universitário Clementino Fraga Filho-Universidade Federal do Rio de Janeiro, Rio de Janeiro, Brasil; [5]Department of Radiology, Kansai Rosai Hospital, Hyogo, Japan; [6]Department of Radiology, Samsung Medical Center, Sungkyunkwan University School of Medicine (SKKU-SOM), Seoul, Korea

Non-infectious granulomatous lung disease represents a diverse group of disorders characterized by pulmonary opacities associated with granulomatous inflammation, a relatively nonspecific finding commonly encountered by pathologists. Some lesions may present a diagnostic challenge because of nonspecific imaging features; however, recognition of the various imaging manifestations of these disorders in conjunction with patients' clinical history, such as age, symptom onset and duration, immune status, and presence of asthma or cutaneous lesions, is imperative for narrowing the differential diagnosis and determining appropriate management of this rare group of disorders. In this pictorial review, we describe the pathologic findings of various non-infectious granulomatous lung diseases as well as the radiologic features and high-resolution computed tomography imaging features.

Keywords: *Non-infectious granulomatosis; Granulomatous lung disease; Lung parenchyma; Radiography; High-resolution computed tomography*

INTRODUCTION

Non-infectious granulomatous lung disease represents a diverse group of disorders characterized by pulmonary opacities associated with granulomatous inflammation, a relatively nonspecific finding commonly encountered by pathologists [1-3]. Granuloma formation is a chronic inflammatory reaction involving the macrophage system and other inflammatory cells. In affected organs, the first manifestation of granuloma is an accumulation of mononuclear inflammatory cells, mostly T cells and

monocyte macrophages [4,5]. The early inflammatory process is followed by the organization of the granuloma, a compact and highly dynamic structure composed of a central cluster of mononuclear phagocytes and epithelioid multinucleated cells, generally surrounded by a rim of lymphocytes [6-9].

Patients with non-infectious pulmonary granulomatosis may initially be identified based on pulmonary symptoms or chest radiographic abnormalities [10-12]. A large variety of non-infectious pulmonary disorders may be associated with occasional granulomatous lesions: 1) inflammatory: sarcoidosis and necrotizing sarcoid granulomatosis (NSG); 2) pulmonary lymphoid lesions: lymphomatoid granulomatosis (LYG); granulomatous-lymphocytic interstitial lung disease (GLILD); 3) aspiration/exposure: aspiration pneumonia, talcosis, berylliosis, and hypersensitivity pneumonitis (HP); 4) vasculitis: granulomatosis with polyangiitis (GPA) (formerly Wegener's granulomatosis) and eosinophilic granulomatosis with polyangiitis (EGPA) (formerly Churg-Strauss syndrome); and 5) collagen vascular disorders: rheumatoid lung nodules.

Diverse and nonspecific findings may be seen on conventional chest radiography. High-resolution computed tomography (HRCT) demonstrates more characteristic patterns and distribution of parenchymal opacities than chest radiography. Although CT findings are often helpful, there is still a considerable overlap of imaging findings among the various forms of non-infectious pulmonary granulomatosis [13,14].

Herein, we describe and illustrate the imaging features of common and uncommon non-infectious granulomatous lung disease and correlate these features with the pathologic findings in order to suggest a specific diagnosis or to substantially narrow the differential diagnosis using the imaging appearance and anatomic location of the lesion.

Pulmonary Inflammatory Lesions

Sarcoidosis

Sarcoidosis is a multisystem granulomatous disorder of unknown origin with worldwide distribution and protean clinical manifestations. It is a global disease with a worldwide incidence of 1–40 cases per 100000 people per year and a prevalence of 0.2–64 cases per 100000 people [15-18]. The disease mainly affects people in the third and fourth decades of life but may also occur in children and elderly subjects. It is characterized by a T-helper response in which CD4 lymphocytes and activated macrophages accumulate in affected organs, resulting in granuloma formation.

Pulmonary involvement is the most common feature, occurring in more than 95% of patients with bilateral hilar lymphadenopathy; multiple organ systems may also be involved [18]. Approximately 30% to 50% of patients are asymptomatic, with bilateral hilar lymphadenopathy detected incidentally on chest radiography. The most common pulmonary complaints are cough, shortness of breath, dyspnea, and bronchial hyperreactivity; constitutional symptoms are common and include fever, fatigue, weakness, malaise, and weight loss [15,16,19]. Although in the majority of patients, pulmonary sarcoidosis follows a benign course and tends to resolve spontaneously, in a significant minority, granulomas evolve to progressive fibrosis. Löfgren's syndrome is a clinically distinct phenotype of sarcoidosis; patients typically experience an acute disease onset usually with fever, and characteristic symptoms of bilateral hilar lymphadenopathy, erythema nodosum, and/or bilateral ankle arthritis or periarticular

inflammation [20,21]. Immune checkpoint blockade has been associated with multiple distinctive side effects termed as immune-related adverse events. The most common pulmonary toxicities of these agents include pneumonitis and sarcoid-like granulomatosis that may be detected during follow-up imaging studies, such as CT or PET/CT [22].

The diagnosis of sarcoidosis is confirmed when typical clinical and radiological findings are supported by histological evidence of non-necrotizing granulomas and exclusion of possible alternative diagnoses [23-26].

The classic histologic findings in sarcoidosis are well-formed, compact, non-necrotizing granulomas often surrounded by concentric layers of hyaline collagen, confined to the interstitial compartment, and distributed in a characteristic lymphangitic pattern [23,27-29]. Sarcoid granulomas are always well-circumscribed interstitial groups of epithelioid histiocytes, multinucleated giant cells, and variable numbers of chronic inflammatory cells. This feature is helpful and is in contrast to the poorly formed granulomas seen in HP [30]. Gross findings comprise variably sized nodules showing a distinctive predilection for bronchovascular bundles, interlobular septa, and visceral pleura. Distribution of granulomas in a lymphangitic pattern is a distinctive feature of sarcoidosis that can be extremely helpful for diagnosis. Infectious granulomas tend to be randomly scattered in the parenchyma, and the granulomas of HP are often centrilobular. Usually, a biopsy is required to demonstrate non-necrotizing granulomas. However, an accurate distinction between different causes of granulomas is, in many cases, not possible.

Parenchymal disease results from interstitial involvement by the granulomatous process leading to irreversible parenchymal changes related to fibrosis. At presentation, the chest radiograph is abnormal in approximately 90% of patients. The most characteristic radiologic findings are symmetric bilateral hilar and right paratracheal lymph node enlargement or diffuse micronodular pulmonary infiltration. Eggshell calcification is thought to develop only in affected nodes and is related to disease duration.

Several HRCT findings have been associated with sarcoidosis, reflecting the histologic findings; small nodules along the bronchovascular bundles, interlobular septa, major fissures, and pleural/subpleural regions represent the typical perilymphatic distribution (Fig. 1) [24,31,32]. Other HRCT signs of sarcoidosis are the reversed halo sign, a focal, rounded area of ground-glass surrounded by an

approximately complete ring of consolidation (Fig. 2) and the galaxy sign, a lung nodule formed by the confluence of multiple small-sized nodules which separate from one another (Fig. 3). Confluence of granulomas may also result in nodules or masses measuring 1–4 cm in diameter. Fibrotic conglomerate masses, reminiscent of those seen in silicosis, may also develop in advanced disease. These findings typically predominate in the middle and upper lung zones [33]. If less characteristic clinical or radiological manifestations predominate, fluorodeoxyglucose (FDG)-FDG-PET, which is highly sensitive in detecting active granulomatous lesions, can be used [34].

Progressive fibrosis and architectural distortion lead to honeycombing, fibrocystic changes, bullae, traction bronchiectasis, and retraction of the pulmonary hila. Air

trapping because of small airway obstruction may also be observed [35]. Superimposed infection of fibrocystic spaces, particularly with Aspergillus, is a frequent complication of sarcoidosis and accounts for significant morbidity and mortality [36-38].

Necrotizing Sarcoid Granulomatosis

NSG is a form of granulomatous lung disease first described in 1973 by Liebow [39] and is characterized by extensive vascular granulomas that infiltrate and occlude pulmonary arteries and veins, accompanied by widespread necrosis of lung tissue. Initially, NSG was considered as a provisional diagnostic term; however, the problem was whether the disease represented necrotizing angiitis with sarcoid reaction or sarcoidosis with necrosis of the
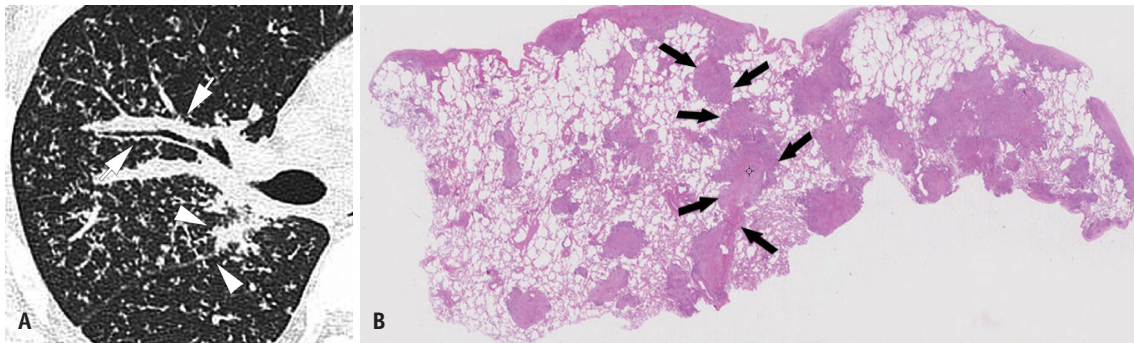

Fig. 1. Sarcoidosis in 51-year-old male (perilymphatic pattern).
A. Close-up view of an axial CT scan shows sparse micronodules with a typical perilymphatic distribution, especially along the fissures (arrowheads) and bronchovascular bundles (arrows). **B.** Low-power scanning magnification demonstrates the lymphangitic distribution of granulomas involving bronchovascular bundles, pleura, and interlobular septa typical of sarcoid (arrows). These findings correlate with the CT appearance (hematoxylin and eosin stain, X 40).
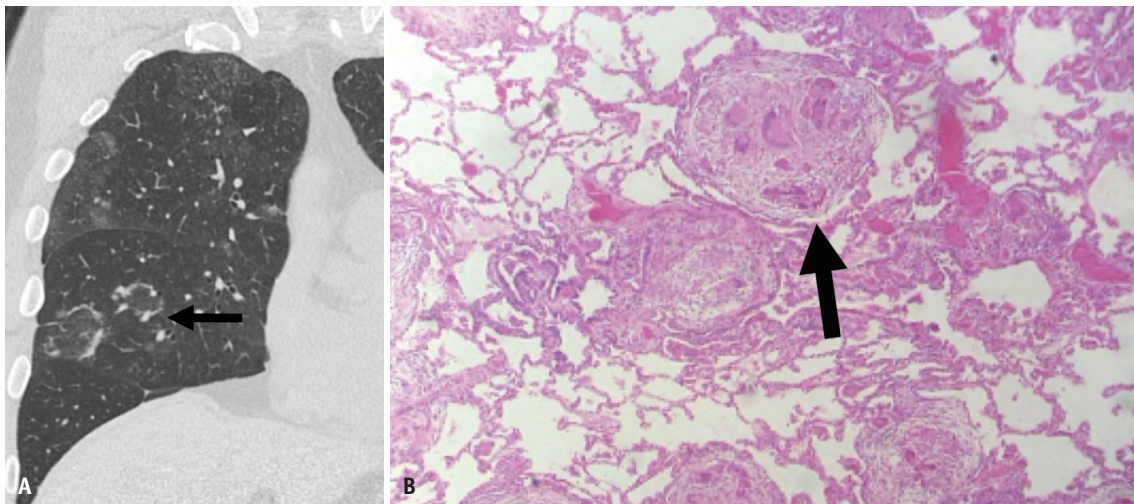

Fig. 2. Sarcoidosis in 28-year-old female (reversed halo sign).
A. Close-up view of a coronal CT scan shows two central ground-glass opacities surrounded by a more or less complete ring of consolidation (reversed halo sign) (arrow). **B.** Medium power magnification demonstrates the compact, well-circumscribed non-necrotizing granulomas containing multinucleated giant cells typical of sarcoid (arrow) (hematoxylin and eosin stain, X 200).

granulomas and the vessels [40-43]. Granulomatous pulmonary angiitis is a nonspecific lesion observed in a variety of conditions, including Wegener's granulomatosis, NSG, chronic beryllium disease (CBD), foreign body embolization in drug abusers, and schistosomiasis [44]. NSG no longer qualifies as a separate entity [42]. The term "sarcoidosis with NSG pattern" should be used in place of NSG to reflect the clinical entity of nodular sarcoidosis [45].

Although the clinical presentation is variable, the majority of patients present with respiratory and systemic symptoms and nodular lung lesions simulating metastatic or primary lung neoplasms. Cough is the most common clinical manifestation, followed by chest pain, dyspnea, fever, and constitutional symptoms of weight loss and fatigue. Patients with NSG have no upper airway disease, glomerulonephritis,

or systemic vasculitis; extrapulmonary involvement has been observed in 20% to 30% of cases [46,47].

The histopathologic features of pulmonary NSG show sarcoid-like granulomas with central necrosis and granulomatous vasculitis [44,46,48].

The predominant radiologic findings were multiple round or oval pulmonary nodules without a specific relationship to lobular structures and interlobular septa. A uniform or random distribution throughout the lungs and a relationship with pleural surfaces and fissures are common. The nodule margin is most often well defined. Cavitation may be seen on follow-up CT images [49].

Multiple large nodular lesions, seen in 1.5% to 4% of patients, are a rare manifestation of pulmonary sarcoidosis (Fig. 4) [50].
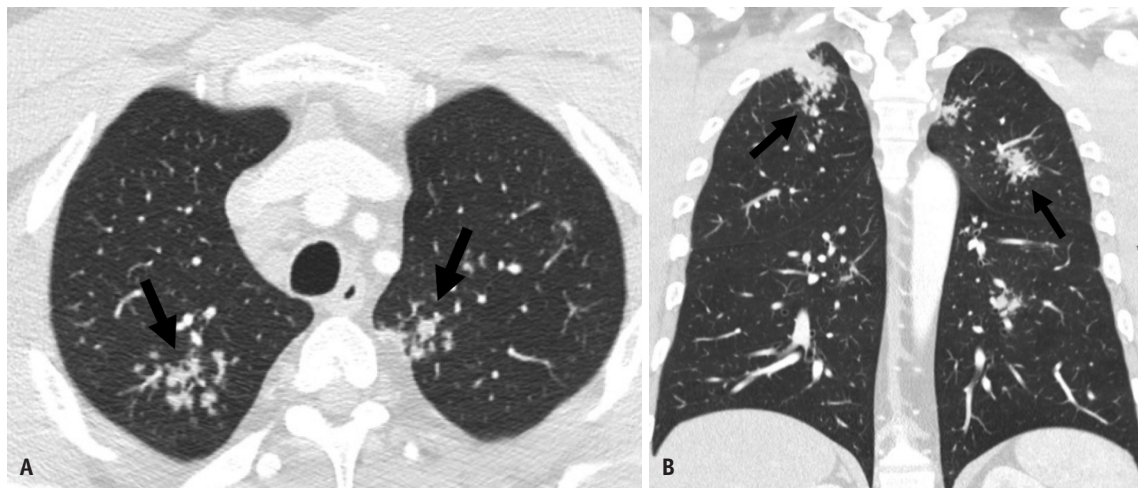

Fig. 3. Sarcoidosis in 40-year-old male (galaxy sign).
A, B. Axial **(A)** and coronal **(B)** CT images show multiple upper lobe–predominant solid pulmonary nodules surrounded by tiny satellite micronodules 1–2 mm (arrows).
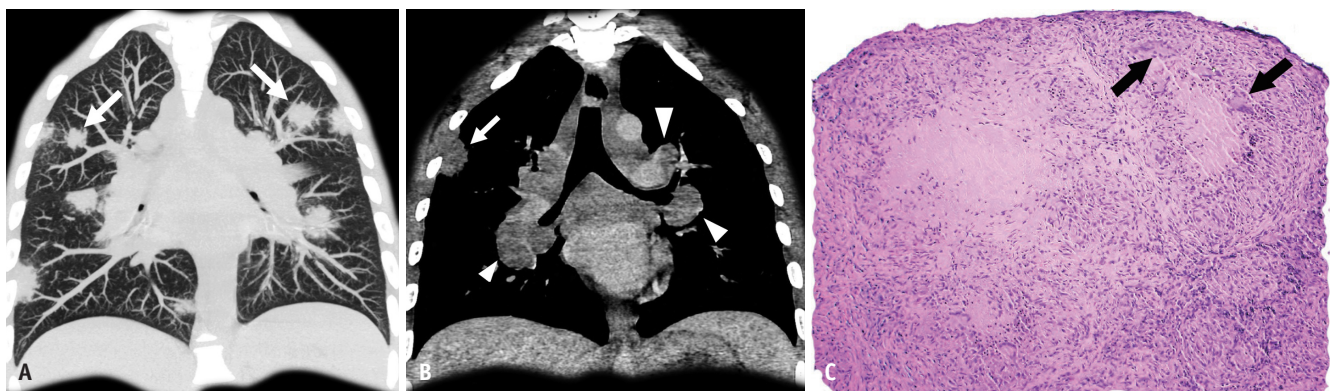

Fig. 4. Necrotizing sarcoid granulomatosis.
A. Coronal (MIP reformatted image) chest CT shows bilateral nodular opacities with irregular borders (arrows). **B.** Coronal (minIP reformatted image) chest CT shows hypodense nodules (arrow). Mediastinal and hilar adenopathies are also seen (arrowheads). **C.** Medium-power magnification demonstrates a conglomeration of necrotizing (pale eosinophilic hypocellular zones) granulomas with scattered multinucleated giant cells (arrows) compatible with "sarcoidosis with necrotizing sarcoid granulomatosis pattern" that correlates with nodules and masses seen on chest CT (hematoxylin and eosin stain, X 40).

Pulmonary Lymphoid Lesions

Lymphomatoid Granulomatosis (LYG)

LYG is a very rare Epstein-Barr virus (EBV)-driven lymphoproliferative disease involving extra-nodal sites and is composed of EBV-positive B cells admixed with reactive T cells, which usually predominate [51-55]. In the current WHO classification, LYG is grouped along with NHL as a neoplasm of mature B cells [56]. Histologically, LYG shows an angiocentric and angiodestructive accumulation of heterogeneous polymorphous group of T cells with varying numbers of atypical clonal EBV-positive B cells around the muscular arteries and veins, with the invasion of these vessels and areas of necrosis presenting later in the disease process [51,57].

Pulmonary involvement occurs in > 90% of patients and is usually present at initial diagnosis. The clinical behavior of LYG varies widely; the disease ranges from an indolent process, which may result in spontaneous remission, to an aggressive large B-cell lymphoma. Predisposing conditions include patients with an underlying acquired or inherited immunodeficiency syndrome (e.g., Wiskott Aldrich syndrome, X-linked lymphoproliferative syndrome, HIV/AIDS, allogeneic organ transplantation) or autoimmune diseases (e.g., Sjögren syndrome, rheumatoid arthritis, sarcoidosis, ulcerative colitis, and common variable immunodeficiency). LYG can lead to progressive pulmonary failure, central nervous system disease, or progression to overt EBV-positive lymphoma.

The most common radiologic and CT features observed in approximately 80% of all cases are unilateral or bilateral multiple lung nodules 0.5–8 cm in diameter with a peribronchovascular distribution and basal predominance (Fig. 5) [58]. The lesions can progress rapidly, coalesce, and cavitate (Fig. 6). Nodules can disappear or migrate spontaneously, and a "reversed halo sign" is frequently observed [59,60]. Mediastinal lymph node enlargement is rare. Pleural effusion is sometimes present. FDG PET-CT shows avid FDG uptake in these lesions [61].

Common Variable Immunodeficiency (CVID)/ Granulomatous-Lymphocytic Interstitial Lung Disease (GLILD)

Common variable immunodeficiency is a primary immunodeficiency of unknown etiology that leads to a clinical syndrome with low levels of serum immunoglobulins and an inability to make specific antibodies [62,63]. CVID is characterized by recurrent bacterial infections, particularly in the respiratory tract, and due to defects in cellular immunity, CVID may also predispose to opportunistic infections [64,65]. Secondary causes of decreased serum immunoglobulin levels must be ruled out in any patient that meets the diagnostic criteria for CVID [66]. A CT scan at the time of diagnosis can identify bronchiectasis, interstitial lung disease, and granulomatous lung disease, even in asymptomatic patients. Follow-up chest CT should
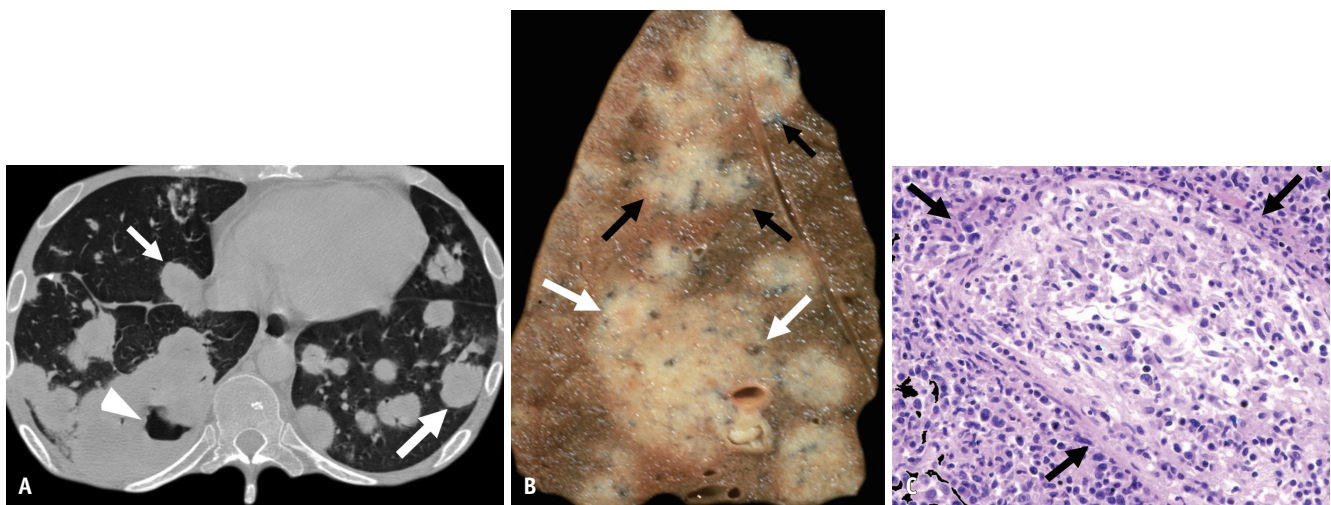

Fig. 5. Lymphomatoid granulomatosis a 56-year-old female.
A. Axial pre-contrast CT image demonstrates multiple pulmonary nodules and masses (arrows). Nodules and masses are distributed along bronchovascular bundle and in subpleural region. Large mass in the right lower lobe is cavitary (arrowhead). **B.** Autopsy gross specimen shows multiple ill-defined yellowish nodules (black arrows) that coalesce leading to large masses (white arrows). **C.** High-power magnification demonstrates vessel wall destruction by marked infiltrates of small Tlymphocytes that obscure malignant large B-lymphocytes seen in lymphomatoid granulomatosis (arrows) (hematoxylin and eosin stain, X 400).

be used judiciously because of the malignancy risk [66,67].

Approximately 10–30% of patients with CVI develop clinical evidence of a non-infectious multisystemic lymphoproliferative disease, which includes diffuse adenopathy, splenomegaly, and granulomatous inflammation in a variety of organs. While airway diseases include infection, obstructive disease, and bronchiectasis, interstitial lung diseases include granuloma, organizing pneumonia, and lymphoid infiltrative disease [66]. Pathologically, it is characterized by both granulomatous and lymphoproliferative histologic patterns [68]. Imaging findings consist of bronchiectasis (cylindrical, varicoid, or cystic), mucoid impaction, and airway thickening [69-72].

The presence of bronchiectasis has been correlated with abnormal CD4^{+} T cell levels [73].

The term GLILD has been used to describe lymphoid parenchymal proliferation that usually consists of noncaseating granulomas, lymphocytic interstitial pneumonia, peribronchiolar lymphoid proliferation (follicular bronchiolitis), and lymphoid hyperplasia [74]. Organizing pneumonia has also been sometimes considered a part of GLILD [62,75]. Typical CT imaging findings include solid nodules (< 3 cm), semisolid nodules, pure ground-glass opacities, enlarged thoracic (hilar and/or mediastinal) lymph nodes, and splenomegaly (Fig. 7) [76].
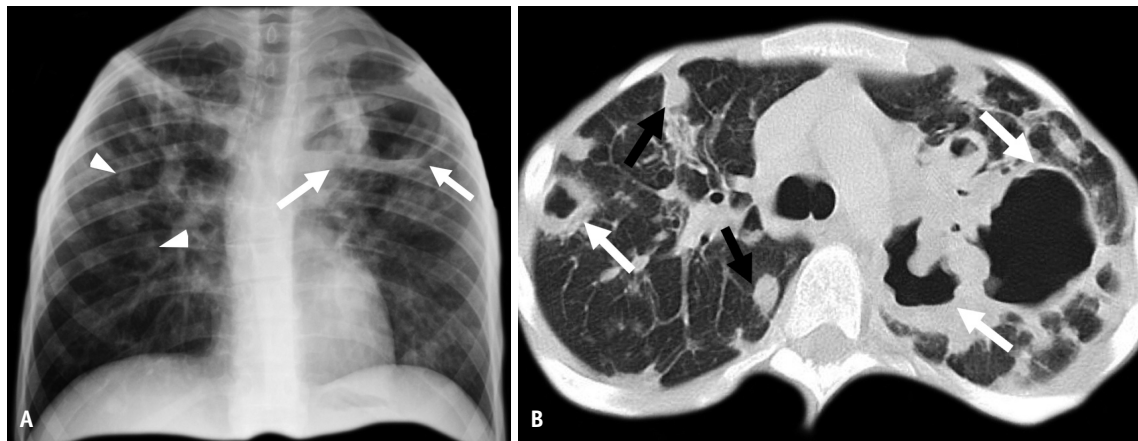

Fig. 6. Lymphomatoid granulomatosis a 62-year-old male.
A. Posteroanterior chest imaging shows a large cavitary mass in the left upper lobe (arrows). Ill-defined randomly distributed rounded opacities are iobserved in the rest of the lung parenchyma (arrowheads). **B.** Corresponding axial chest CT scan shows multiple rounded peripheral solid (black arrows) or cavitary nodules (white arrows).
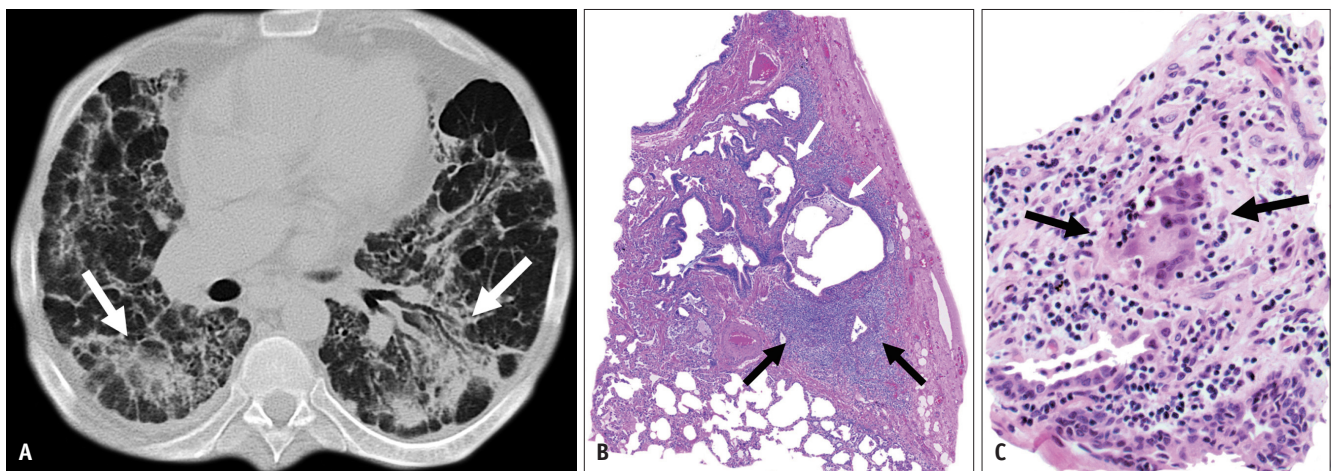

Fig. 7. Granulomatous-lymphocytic interstitial lung disease.
A. Axial chest CT scan shows multiple peripheral and peribronchovascular ground-glass and consolidation (arrows). **B.** Low-power scanning magnification of lung demonstrates airway centered marked infiltrates of chronic inflammatory cells (black arrows) that results in cystic remodeling of distal small airways (white arrows) (hematoxylin and eosin stain, X 40). **C.** High-power magnification demonstrates poorly formed collection of histiocytes and a multinucleated giant cell (arrows). The airway centered lung injury correlates with the peribronchovascular ground glass and consolidation seen on the chest CT (hematoxylin and eosin stain, X 200).

Aspiration/Exposure

The term aspiration describes a variety of situations involving the intake of solid or liquid materials into the airways and lungs [77,78]. Aspiration may occur from exogenous or endogenous gastric sources. The development of aspiration-related pulmonary syndrome depends on the quantity and nature of the aspirated material, chronicity, and host responses [79]. Alcoholism is probably the most important predisposing factor for pulmonary aspiration in adults, although other factors (e.g., general anesthesia, loss of consciousness, structural abnormalities of the pharynx and esophagus, neuromuscular disorders, and deglutition abnormalities) may also contribute to aspiration [78,80-82].

Aspiration Pneumonia

Pulmonary aspiration of gastric contents is a significant cause of morbidity and mortality and is the most common cause of pneumonia [77,81]. Predisposing factors, such as neurologic disorders, structural abnormalities of the pharynx and esophagus, emergency surgical procedures, and dementia are frequently associated with this condition [77]. The most common radiographic pattern is that of bronchopneumonia with scattered air-space opacities. CT has been regarded as the imaging modality of choice for the evaluation of suspected esophagopleural fistula, because the site of communication between the pleural space and the esophagus can often be seen (Fig. 8). Aspiration of leguminous vegetables can cause a granulomatous pneumonitis know as lentil aspiration pneumonia. Typically manifesting as diffuse, ill-defined, small 1–3 mm nodular areas of increased opacity representing the bronchiolar

distribution of the aspirated material [83]. On HRCT, lentil aspiration pneumonia manifests as centrilobular nodules, some with a tree-in-bud appearance [81]. Material from repeated aspirations may appear as disseminated miliary nodules representing inflammation with foreign body reaction in bronchioles, ducts, and alveolar sacs [77,83].

Histologically, aspiration pneumonia is classically characterized by acute inflammation and necrosis centered on bronchioles with remnants of aspirated vegetable material surrounded by multinucleated giant cells [83,84].

Talcosis

Talc (hydrous magnesium silicate) is a mineral widely used in the ceramic, paper, plastics, rubber, paint, and cosmetic industries. The term "talc" is used not only for pure magnesium silicate but also for a mixture of minerals with various other products [85,86].

Pulmonary talcosis should be suspected in patients with a known history of occupational exposure or drug addiction. The causes of pulmonary talcosis may include inhalation of pure talc, inhalation of talc in association with silica (talcosilicosis), or inhalation of talc in association with asbestos fibers (talcoasbestosis). Intravenous injection of talc (intravascular talcosis) occurs most often during recreational drug use when the drug is crushed, melted, dissolved in water, and IV-injected.

History of occupational exposure or drug addiction is the major clue to diagnosis [87-91]. Clinically, patients with pulmonary talcosis can range from asymptomatic to severe disease [92]. A wide variety of pulmonary complications, including asthma exacerbation, barotrauma, hilar lymphadenopathies, and bullous emphysema, may be
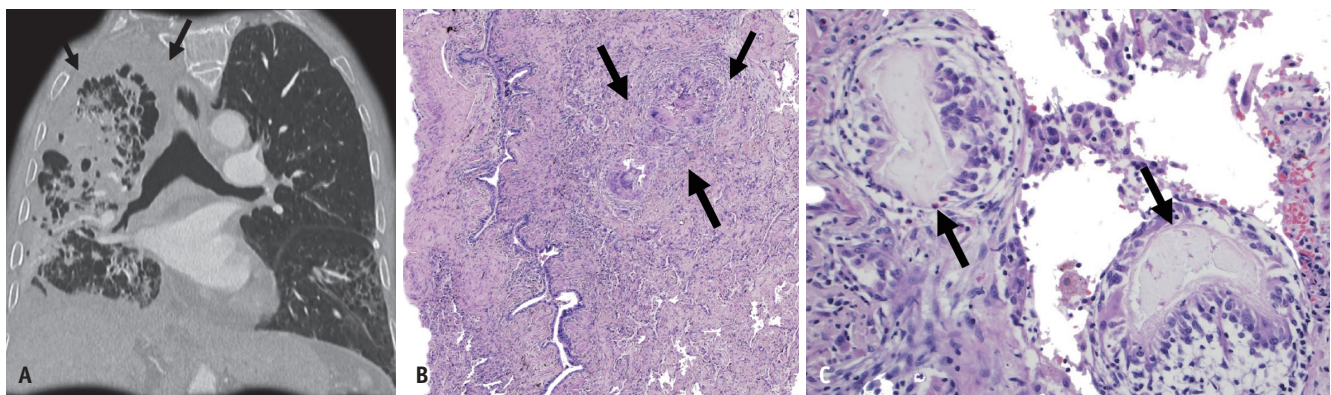
Fig. 8. Aspiration pneumonia in 72-year-old male smoker.
A. Coronal reformatted contrast-enhanced CT shows right upper lobe heterogeneous consolidation and a large empyema (arrows). **B.** Medium-power magnification of lung shows airway centered fibrosis containing two clusters of multinucleated giant cells (arrows) (hematoxylin and eosin stain, X 40). **C.** On high-power magnificent in the right histologic image, the multinucleated giant cells and organizing pneumonia surround fragments of plant material (arrows) (hematoxylin and eosin stain, X 400).

associated with the inhalation of talc, silica, and lactose [93]. The majority of patients usually present with nonspecific complaints, including progressive exertional dyspnea and cough [93,94]. Late complications include interstitial pneumonitis, fibrosis, emphysema, pulmonary arterial hypertension, cor pulmonale, and lung cancer [95-98].

Whether inhaled or injected, talc causes non-necrotizing granulomatous inflammation. In the early stages of the disease, talcosis consists of multiple, small, foreign body granulomas composed of multinucleated cells containing birefringent crystals, which are identified in the alveolar septa and air spaces [11,99]. As the disease progresses, the granulomas can become confluent, resulting in heterogeneous conglomerate masses. Microscopic examination under polarized light shows birefringent needle-shaped talc crystals in multinucleated giant cells and macrophages. These features differ from those seen after intravenous talc injection where the talc particles are larger and become trapped within pulmonary arterioles and

capillaries resulting in thrombosis, vascular and perivascular fibrosis, and chronic inflammation; intravascular and perivascular granulomas can be seen.

In early-stage disease, radiologic diagnosis of pulmonary talcosis is difficult because the findings are often minimal or nonspecific, consisting of extremely tiny, round opacities diffusely distributed throughout both lungs [100]. Earlier thin-section CT findings show a diffuse micronodular pattern with well-defined centrilobular nodules or diffuse ground-glass opacities (Fig. 9); apices and costophrenic sulci are generally spared. In more advanced disease, thin-section CT shows progressive massive fibrosis associated with lower lobe emphysema and diffuse reticulonodular changes [101]. Although CT findings in advanced talcosis are similar to those reported in silicosis, conglomerate masses with areas of high attenuation usually involve the upper lung zones in silicosis, while in talcosis, they are distributed throughout all lung zones [11,100].
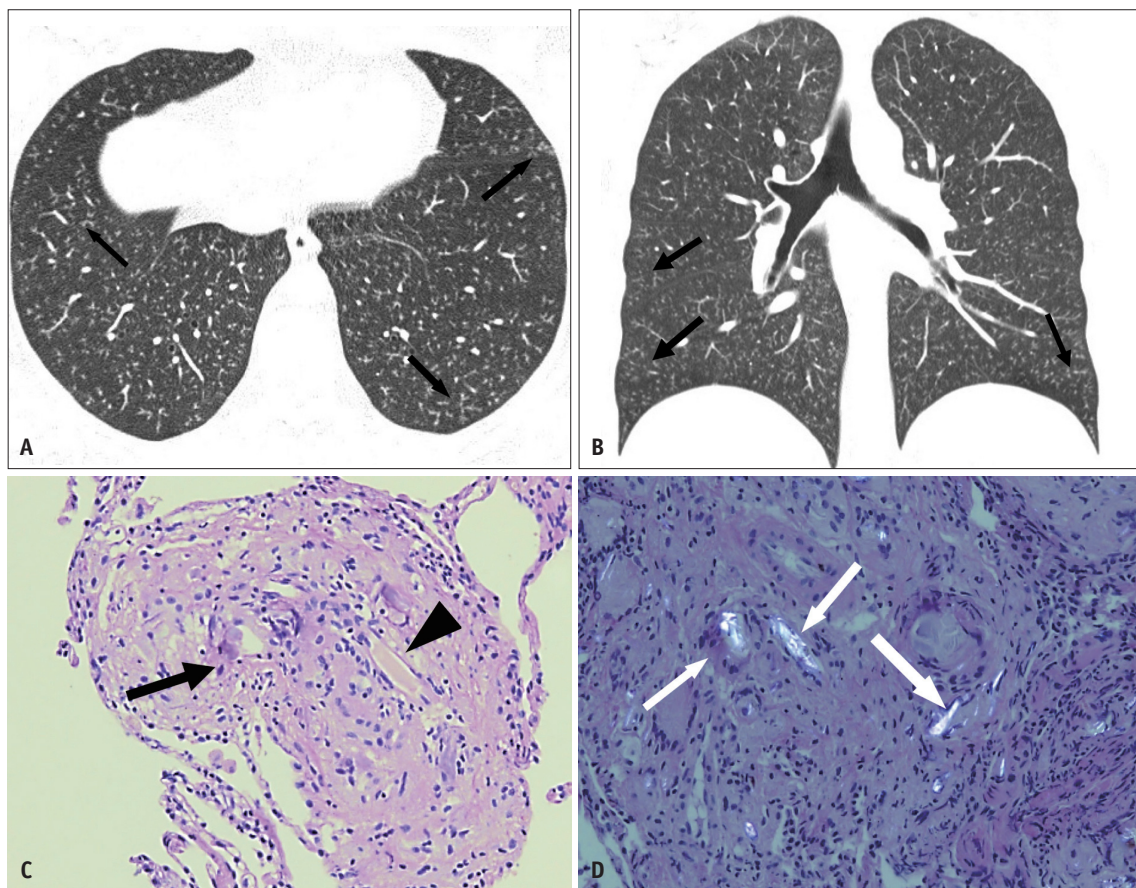
Fig. 9. Talcosis.
A, B. Axial and coronal reformatted CT images show numerous small bilateral centrilobular nodules, associated with a tree-in-bud pattern (arrows). **C.** Lung tissue biopsy demonstrates an interstitial granulomatous reaction to the talc particles (arrowhead) with a giant-cell reaction (arrow) (hematoxylin and eosin stain, X 400). **D.** Under polarized light, birefringent crystals are visible (arrows) (hematoxylin and eosin stain, X 400).

Berylliosis

Beryllium is a naturally light-weight metal extracted from ores and processed into metal, oxides, alloys, and composite materials [102]. The major applications are in automotive electronics, telecommunications, computers, aerospace, ceramics, fluorescent lamps and neon lights, and dentistry and dental supplies [103-105].

Berylliosis, a granulomatous disorder caused by exposure and inhalation of dust, fumes, or aerosols of beryllium metal or its salts, is characterized by the accumulation of CD4^{+} T cells and macrophages in the lower respiratory tract [86].

The clinical course varies with the intensity and chronicity of exposure, and patients can range from asymptomatic to those with severe disease [106,107]. Symptoms usually include dyspnea, cough, fever, anorexia, and weight loss [108]. Pulmonary function testing shows restriction with diminished diffusing capacity. There are two distinct types of lung injury related to beryllium exposure: 1) acute beryllium pneumonitis caused by direct acute lung injury resulting from the inhalation of high levels of beryllium particles and 2) CBD caused by delayed-type hypersensitivity developed months or years after exposure. CBD may be nearly radiographically indistinguishable from sarcoidosis; current workplace protection has virtually eliminated acute disease [109,110]. CBD continues to occur in the nonoccupational setting and among bystanders in industry, masquerading as sarcoidosis [111].

Histologically, well-formed non-necrotizing granulomas are seen in a lymphatic distribution involving bronchovascular bundles, pleura, and interlobular septa indistinguishable from other granulomatous disorders, such as sarcoidosis [112]. Confluence of numerous interstitial granulomas can result in large, irregular, mass-like opacities. Environmental exposure history may help distinguish between pneumoconioses and sarcoidosis [113].

In the early stage of the disease, minimal or no visible abnormalities may be observed on chest radiographs, although thin-section CT scans demonstrate thickened intralobular and interlobular lines [114,115].

Chest radiography is often normal in early-stage disease but disease progression depicts small nodules and reticulation, typically with predominant distribution in the middle and upper lung (early) [115]. Reticulation, architectural distortion, honeycombing, and mass-like lesions are observed because of the coalescence of small nodules and lymphadenopathy [115,116].

Characteristic CT findings include the presence of small nodules (< 3 mm) in a perilymphatic distribution and nodular thickening along the lymphatics in the bronchovascular sheath and, to a lesser extent, in the interlobular septa and subpleural lung regions (Fig. 10) [86,115].

Hypersensitivity Pneumonitis

HP, one of the most common diffuse parenchymal lung diseases, is an immunologically mediated diffuse lung disease characterized by a complex immunological reaction of the lung parenchyma in response to repetitive inhalation of a sensitized allergen [117,118]. The severity of the disease and clinical presentation varies depending on the inhaled antigen and quantity. It has been conventionally classified into acute, subacute, and chronic forms based on the time course and presentation. Chronic HP is a fibrotic lung disease resulting from long-term exposure to an offending antigen [119].

More recently, the results of a cluster analysis were compared with the classical classification of HP [120]. Results suggest that patients with HP should be classified into only one of the two categories (Cluster 1 and Cluster 2)

Fig. 10. Berylliosis in a 49-year-old male who worked for 7 years in metal polishing.
A, B. Axial thin-section CT scans (1.0-mm-thick-sections) obtained at the levels of the bronchus intermedius **(A)**. At the basal segmental bronchus shows multiple small nodules along the bronchovascular bundles (straight arrows) and in subfissural regions (arrowheads) and enlarged hilar lymph nodes (curved arrows) **(B)**. **C.** High-power magnification of a pathologic specimen obtained with mediastinoscopic lymph node biopsy shows multiple noncaseating granulomas (arrows) (Courtesy of Chong S) (hematoxylin and eosin stain, X 400).

based on clinical evaluation, pulmonary function tests, and HRCT findings. In Cluster 1, patients would present with recurrent systemic symptoms (chills and body aches) and tightness of the chest occurring a few hours after antigen exposure, inspiratory crackles would be frequent, and chest X-rays would be normal in almost 30% of the cases. In Cluster 2, patients would present with features of advanced interstitial lung disease, clubbing, inspiratory crackles, a restrictive pattern on pulmonary function tests, and resting hypoxemia. One-third of the patients showed fibrotic

Fig. 11. Subacute or cluster 1 hypersensitivity pneumonitis.
Axial thin-section CT scan at the level of lung bases shows diffuse ground-glass opacity interposed with areas of normal lung and lobular areas of decreased attenuation (arrows).

changes on HRCT [120].

Histologic studies in acute HP are scanty, as lung biopsy is generally not necessary for diagnosis. The histologic changes of subacute HP occur at the level of the terminal bronchioles and consist of a classic histologic triad of a lymphocytic interstitial infiltrate, organizing pneumonia, and poorly formed non-necrotizing granulomas [121]. Typical granulomas are present in approximately 80% of surgical biopsies and consist of loose collections of histiocytes or scattered giant cells. Necrosis is not a component of the granulomatous reaction in cases of HP [122]. A mild perivascular lymphoid accumulation is typically present in HP, but prominent germinal centers or dense lymphoplasmacellular infiltration along vascular sheaths are not typical and should raise concern for lymphoproliferative disease [121]. Chronic HP can appear like usual interstitial pneumonia (UIP) on histology, but it is distributed in the upper lobes rather than the lower lobes as in UIP/IPF. The characteristic HRCT findings of acute and subacute HP are characterized by ground-glass attenuation with poorly defined centrilobular nodular opacities (Fig. 11), thin-walled cysts, and mosaic perfusion (focal areas of air trapping) (Fig. 12) [123]. Coexisting thin-walled cysts have been reported in 13% of the patients with subacute HP and are believed to be caused by partial bronchiolar obstruction by peribronchiolar lymphocytic infiltration [124]. Chronic HP has a bronchovascular distribution
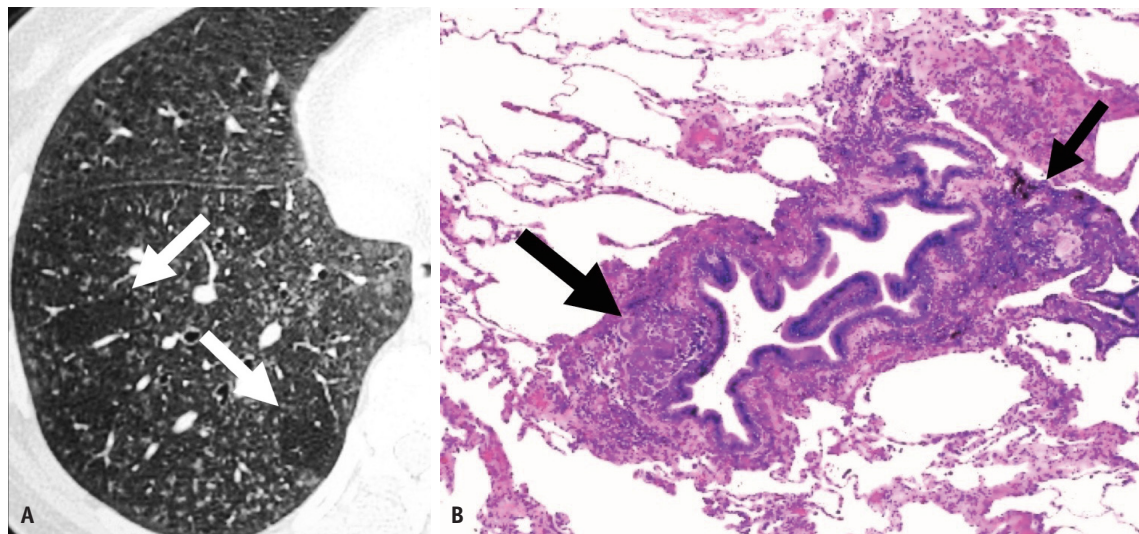

Fig. 12. Subacute or cluster 1 hypersensitivity pneumonitis.
A. Close-up view of thin-section CT scan at the level of the right-lower lobe shows diffuse ground-glass opacities and poorly defined centrilobular nodules (arrows). Note lobular areas of decreased attenuation and vascularity reflecting air trapping (arrows). **B.** Medium-power magnification of lung demonstrates airway centered chronic inflammation containing poorly formed granulomata (arrows). The chronic inflammatory infiltrates surrounding small airways correlate with the centrilobular nodules and mosaic attenuation seen on the CT axial image **A** (hematoxylin and eosin stain, X 200).

of fibrosis, reticular pattern, air trapping, and traction bronchiectasis (Fig. 13) [125,126]. Importantly, subacute and chronic HP may mimic several interstitial lung diseases, including nonspecific interstitial pneumonia and UIP, making diagnosis extremely difficult because of the overlap of the clinical history, and the functional and imaging findings [127-129]. The best diagnostic approach is to integrate clinical, radiological, and pathological information at a multidisciplinary team meeting.

Vasculitis

Granulomatosis with Polyangiitis (GPA)

GPA, formerly termed Wegener's granulomatosis, is an antineutrophil cytoplasmic autoantibodies (ANCA)-associated systemic vasculitis typically involving the upper respiratory tract, lower respiratory tract (bronchi and lungs), and kidneys, with varying degrees of disseminated vasculitis [39,130].

The spectrum and severity of GPA are heterogeneous, ranging from an indolent disease involving only one site to fulminant, multi-organ vasculitis leading to death [131]. The disease classically presents with upper and lower respiratory tract symptoms and renal involvement. Pulmonary involvement occurs in 55–90% of patients. Clinical pulmonary manifestations include cough, dyspnea, impaired pulmonary function, bronchostenosis, and diffuse alveolar hemorrhage [131-133].
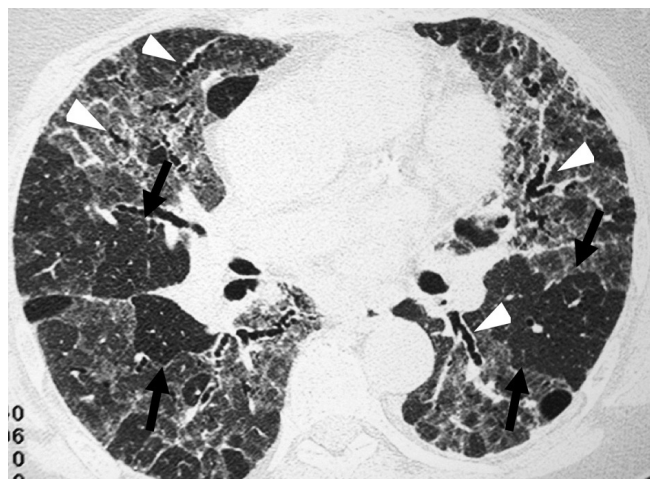

Fig. 13. Chronic or cluster 2 hypersensitivity pneumonitis.
Typical CT findings of biopsy-proven chronic hypersensitivity pneumonitis in a bird breeder. High-resolution CT scans show mild reticulation with superimposed patchy ground-glass opacities and traction bronchiectasis and bronchiolectasis (white arrowheads). Lobular areas of decreased attenuation and vascularity (black arrows) are also present.

GPA has many histopathological features. The microscopic hallmark is a triad of parenchymal necrosis, vasculitis, and granulomatous inflammation. The major histopathologic features of GPA are those generally regarded as the diagnostic criteria: parenchymal necrosis, vasculitis, and granulomatous inflammation accompanied by a mixed infiltrate of neutrophils, lymphocytes, plasma cells, macrophages, giant cells, and eosinophils [134]. Less frequent features not representing diagnostic criteria are alveolar hemorrhage, organizing intraluminal fibrosis, lymphoid aggregates, tissue eosinophils, xanthogranulomatous lesions, alveolar macrophage accumulation, and organizing pneumonia-like fibrosis [133,135]. The diagnosis ultimately relies on a constellation of radiographic and pathologic findings, laboratory values, and accurate clinical history [136].

GPA in the thorax presents with a wide variety of radiologic findings [137-140]. Chest radiographs are abnormal in 70% of the patients during the course of the disease. Lesions can be single or multiple (usually < 10 lesions) and range in size from a few millimeters to over 10 cm. Common pulmonary radiologic findings include bilateral waxing and waning nodules and masses, cavitation in nodules larger than 2 cm with a thick wall and irregular inner lining, ground-glass opacities, and consolidations (Fig. 14) [140]. Pleural effusion can result from primary involvement or secondary to renal failure.

The characteristic CT manifestations consist of bilateral subpleural or peribronchovascular nodules or masses (1–4 cm in diameter), sometimes spiculated; in approximately 50% of the cases, the masses may cavitate [140,141]. Nodules with feeding vessels and wedge-shaped lesions abutting the pleura are less frequent findings. In unusual cases, the disease may manifest itself as a solitary lung lesion that can measure up to 10 cm in diameter [142]. In up to 50% of patients, bilateral nonsegmental or peribronchovascular areas of airspace consolidation, peribronchial thickening, small centrilobular nodules, and branching linear structures (so-called tree-in-bud pattern) are frequently seen [138,143]. Ground-glass opacities and airspace consolidation correlate with focal or diffuse pulmonary hemorrhage that occurs in approximately 10% of patients [138,140,142,144-146]. Histologically, pulmonary hemorrhage may result in areas of organizing pneumonia-like reactions (Fig. 15) [147]. Calcification within areas of consolidation, although rare, has also been described [148]. Moreover, GPA associated with abnormal pulmonary
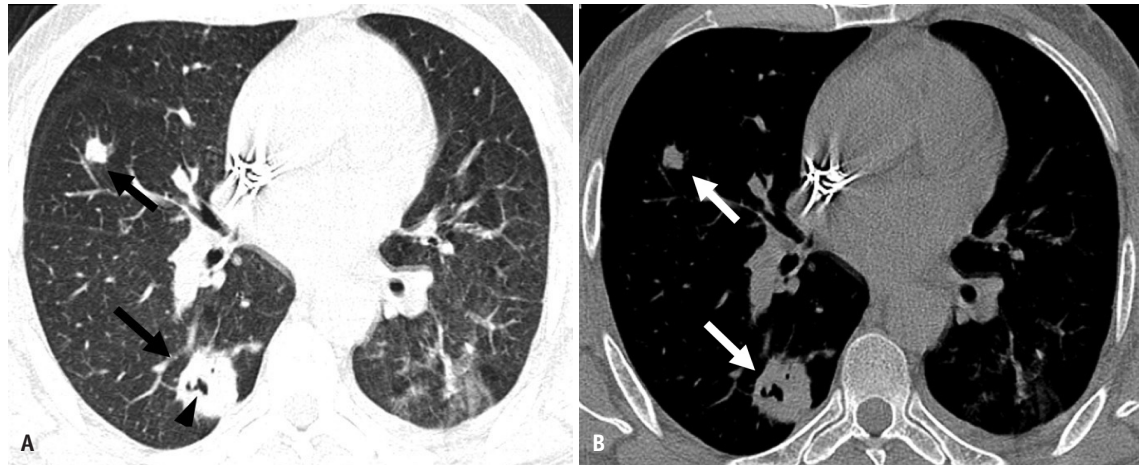
Fig. 14. Granulomatosis with polyangiitis in a 68-year-old male.
A, B. Axial thin-section CT scan at the level of lung bases (lung window) **(A)** and **(B)**, mediastinal window show two rounded opacities of different sizes in the lateral segment of the middle lobe and in the superior segment of the right lower lobe (black arrows in **A**; white arrows in **B**); largest nodule shows central cavitation with thick walls and irregular inner margins (blackarrowhead in **A**).
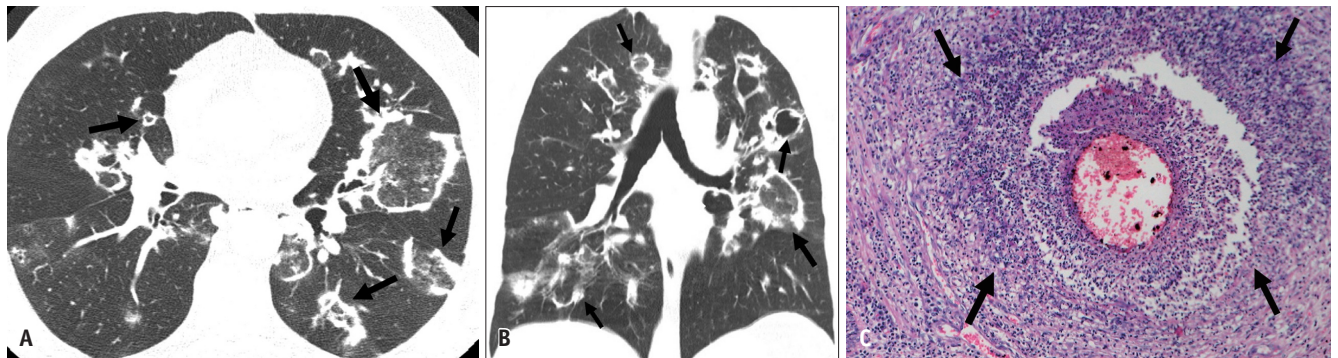

Fig. 15. Granulomatosis with polyangiitis (reversed halo sign).
A, B. Axial **(A)** and coronal **(B)** thin-section CT shows bilateral rounded opacities of different sizes with a central hypodense zone surrounded by a ring of consolidation (reversed halo sign) (arrows). **C.** Medium power magnification of lung demonstrates necrotizing vasculitis evidenced by an arterial wall (arrows) infiltrated and destroyed by neutrophils (hematoxylin and eosin stain, X 400).

perfusion at the subsegmental level results in ischemia or frank infarctions leading to ground-glass opacities representing necrotic cellular infiltrates in the alveoli or mosaic perfusion [140]. Enlarged mediastinal lymph nodes, always seen in association with parenchymal abnormalities, occur in up to 15% of cases [140].

Eosinophilic Granulomatosis with Polyangiitis (EGPA)

The Chapel Hill consensus conference in 1994 defined EGPA (formerly Churg-Strauss syndrome) as eosinophil-rich and granulomatous inflammation involving the respiratory tract and necrotizing vasculitis affecting small to medium-sized vessels, occurring in patients with late-onset asthma and sustained peripheral blood eosinophilia [149].

The American College of Rheumatology criteria for the diagnosis of EGPA include: 1) asthma, 2) peripheral blood eosinophilia greater than 10% of white blood cell differential count, 3) neuropathy, 4) migratory or transient pulmonary opacities, 5) paranasal sinus abnormalities, and 6) tissue eosinophilia [150]. The diagnosis of EGPA can be established if four or more of the previous criteria are present. Asthma is present in almost all patients and usually precedes vasculitis for several years, and is often associated with rhinitis, nasal polyposis, or sinusitis [151]. ANCA are present in approximately 40% of patients. Symptomatic cardiac involvement occurs in as many as 27–47% of cases and is a major contributor to disease-related death in EGPA [152].

Clinically, EGPA occurs mainly in middle-aged adults with various degrees of eosinophilic inflammation and necrotizing vasculitis [153,154]. EGPA typically develops into three sequential phases: 1) prodromal or allergic phase,

usually in the fourth decade, may persist for many years, and is characterized by the occurrence of asthma, allergic rhinitis, and sinusitis; 2) eosinophilic phase, with marked peripheral eosinophilia and eosinophilic organ infiltrations, especially in the lungs, heart, and gastrointestinal system; 3) vasculitic phase, with consequences of a necrotizing vasculitis generally associated with vascular or extravascular granulomatosis and constitutional symptoms, such as fever, malaise, and weight loss [151,155].

There is a spectrum of histopathologic findings of EGPA in the lung. The combination of eosinophilic pneumonia, necrotizing vasculitis, and granulomatous inflammation is considered diagnostic but is infrequently present [156]. Alveolar spaces are often involved in eosinophils, fibrin, organizing fibrosis, and reactive type II pneumocytes. In the absence of vasculitis (clinical or histological), it may be difficult to distinguish between EGPA and other eosinophilic disorders.

The most common radiographic findings consist of bilateral multifocal consolidation, patchy nonsegmental consolidation, and multiple nodules. Less common intrathoracic findings include mediastinal or hilar lymphadenopathy and pleural or pericardial effusion [138,157].

HRCT appearances largely reflect the eosinophilic infiltrate, including migrating patchy infiltrates with a predominantly peripheral distribution, ground-glass opacities, areas of airspace consolidation, centrilobular nodules, and airway abnormalities attributable to asthma [158]. These findings reflect the presence of eosinophilic infiltration of the airspaces, interstitium, airways, and interstitial edema [159]. Interlobular septal thickening may be seen as a result of interstitial edema secondary to cardiac involvement [159]. Histologically, airspace consolidation is due to eosinophils, fibrin, foci of organizing pneumonia, and reactive type II pneumocytes. Up to 25% of patients have few or no imaging abnormalities, and imaging is often of little help in arriving at this somewhat elusive diagnosis (Fig. 16) [160].

Collagen Vascular Diseases

Rheumatoid Lung Nodules

Rheumatoid pulmonary nodules are an uncommon but well-described extra-articular manifestation of rheumatoid disease, occurring most often in cigarette smokers with clinical and radiographic evidence of rheumatoid arthritis [161,162]. The incidence in the lung is approximately 30–40% of cases [163]. Usually, they are multiple and pleural based, and may vary in size from a few millimeters to 7 cm. They may resolve spontaneously, wax and wane in
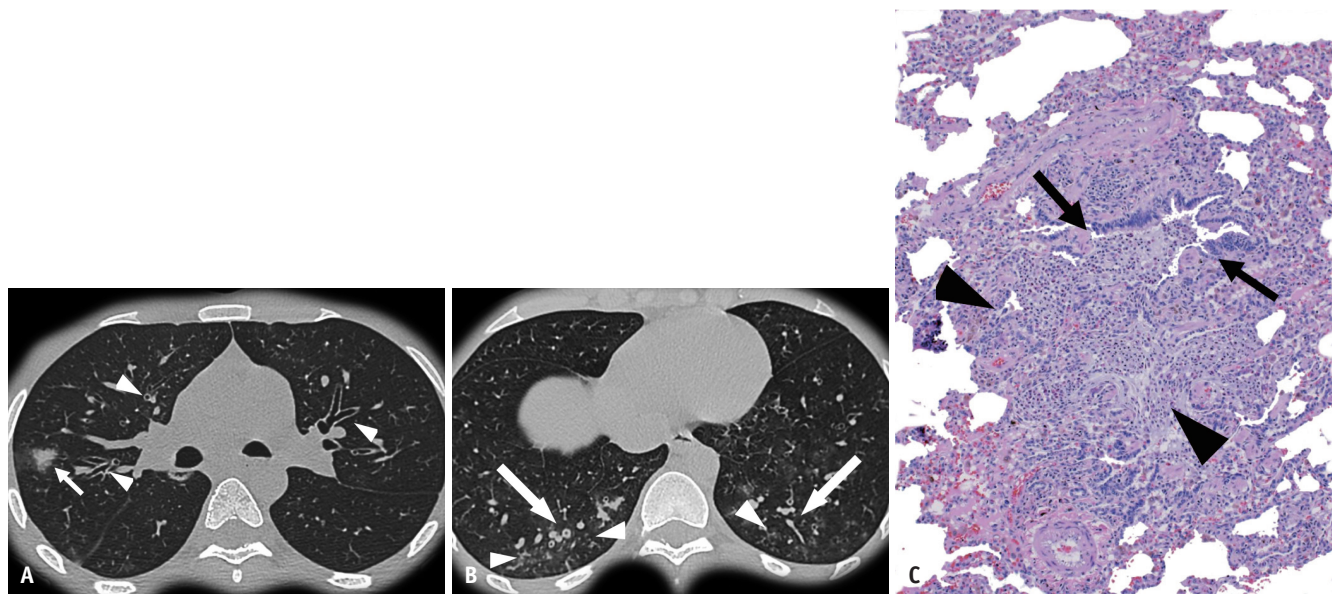

Fig. 16. Eosinophilic granulomatosis with polyangiitis in a 23-year-old male with severe asthma.
A. Axial thin-section CT scan (lung window) at the level of the carina shows an ill-defined nodule surrounded by a halo of ground-glass attenuation (arrow) in the right upper lobe. Note bilateral thickening of bronchial walls (arrowheads). **B.** Axial thin-section CT at the level of lung bases shows bilateral thickening of bronchioles (arrows), mucous plugging and basilar-predominant centrilobular nodules of varying sizes (arrowheads). **C.** Lung biopsy was done through video-assisted thoracic surgery. Low-power magnification shows airway destruction (arrows) with submucosal infiltration and luminal filling with lymphocytes and eosinophils (arrowheads) (hematoxylin and eosin stain, X 400).

concert with the disease activity, or may antedate arthritis [164]. Nodules are typically asymptomatic and require no treatment unless they become quite large, infected, or cavitated. Approximately 50% of rheumatoid pulmonary nodules will cavitate and can sometimes be associated with pleural effusion, pneumothorax, or pyopneumothorax [165,166]. The majority of spontaneous pneumothoraces related to rheumatoid arthritis are associated with subpleural necrobiotic pulmonary nodules [167].

Histologically, necrobiosis with and palisading epithelioid histiocytes is a typical feature. The area of central necrosis contains necrotizing endothelial cells and histiocytes. The outer area tends to show granulation tissue with chronic inflammatory cells and significant stromal fibrosis. Focal vasculitis and occasional giant cells can also be found [168]. Overall, this represents an immune-mediated granulomatous process and shows granulation tissue with chronic inflammatory cells and significant stromal fibrosis [169].
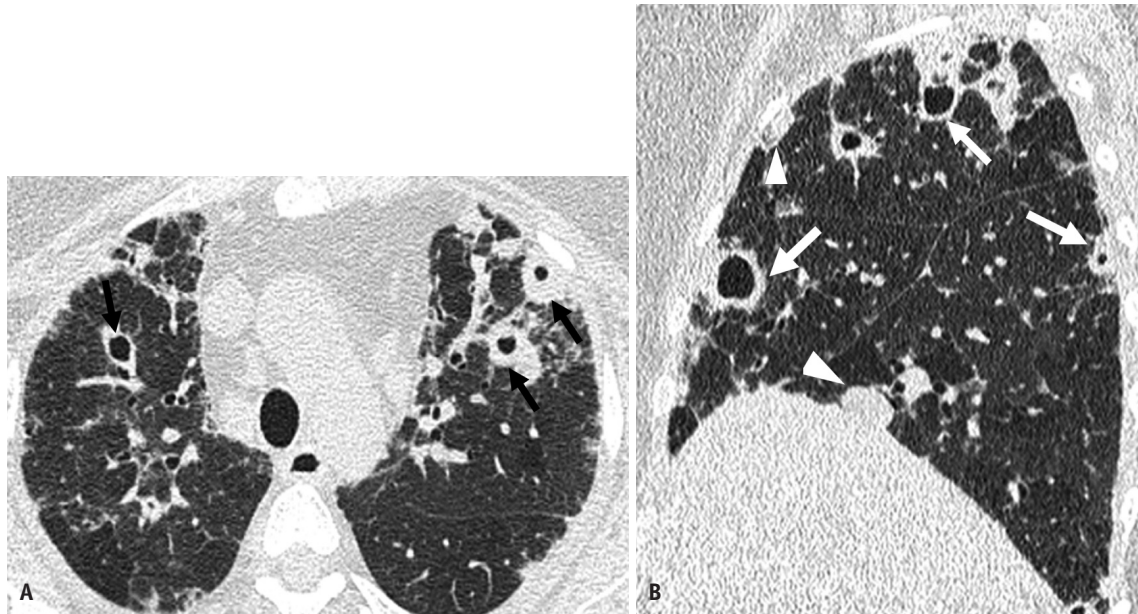

Fig. 17. Rheumatoid nodules.
A, B. Axial **(A)** and sagittal thin-section CT **(B)** images show numerous subpleural pulmonary necrotic (arrows) and solid (arrowheads) necrobiotic pulmonary nodules.
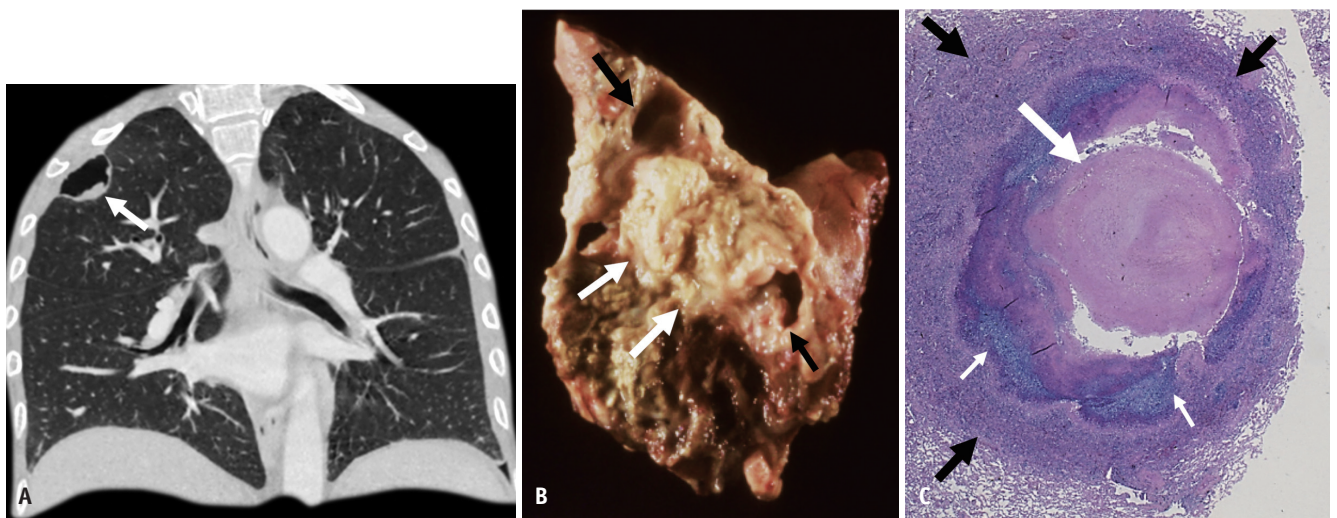
Fig. 18. Rheumatoid nodule.
A. Coronal reformatted contrast-enhanced CT shows a peripheral right upper lobe cavitary mass (arrow). **B.** Surgical gross specimen shows an ill-defined cavitary mass (black arrows) containing necrotic tissue (white arrows). **C.** Low-power scanning magnification of lung demonstrates a necrotizing granuloma with a central zone of necrosis (white arrow) surrounded by a rim of palisading histiocytes (black arrows). The dark blue periphery of the necrotic zone is nuclear debris (small arrows) (hematoxylin and eosin stain, X 40).

CT features more commonly associated with rheumatoid lung nodules consist of multiplicity, smooth border, cavitation, satellite nodules, pleural contact, and a subpleural rind of soft tissue (Figs. 17, 18) [170].

CONCLUSION

The diagnosis of non-infectious pulmonary granulomatosis is difficult because of the variable clinical manifestations and radiologic features. The anatomic distribution of the lesions and radiologic details in conjunction with patients' clinical history is imperative for narrowing the differential diagnosis in order to facilitate proper management.

Author Contributions
Conceptualization: Tomás Franquet, Kyung Soo Lee, Teri J. Franks. Data curation: Ana Giménez, Sandra Mazzini. Formal analysis: Edson Marchiori, Ana Giménez, Sandra Mazzini. Investigation: Sandra Mazzini, Ana Giménez, Edson Marchiori. Methodology: Tomás Franquet, Kyung Soo Lee, Teri J. Franks. Supervision: Jeffrey R. Galvin, Teri J. Franks, Edson Marchiori. Validation: Kyung Soo Lee, Takeshi Johkoh. Writing—original draft: Tomás Franquet, Kyung Soo Lee, Jeffrey R. Galvin. Writing—review & editing: Teri J. Franks, Takeshi Johkoh, Kyung Soo Lee.

ORCID iDs
Tomás Franquet
  https://orcid.org/0000-0002-7443-1730
Edson Marchiori
  https://orcid.org/0000-0001-8797-7380
Ana Giménez
  https://orcid.org/0000-0002-3898-0652
Sandra Mazzini
  https://orcid.org/0000-0002-2619-2253
Takeshi Johkoh
  https://orcid.org/0000-0003-1237-2349
Kyung Soo Lee
  https://orcid.org/0000-0002-3660-5728

REFERENCES

1. Myers JL, Tazelaar HD. Challenges in pulmonary fibrosis: 6 · Problematic granulomatous lung disease. *Thorax* 2008;63:78-84
2. Ohshimo S, Guzman J, Costabel U, Bonella F. Differential diagnosis of granulomatous lung disease: clues and pitfalls: number 4 in the series "pathology for the clinician" edited by Peter Dorfmüller and Alberto Cavazza. *Eur Respir Rev* 2017;26:170012
3. Freundlich IM, Capp MP. Granulomatous disease of the lungs. *Radiol Clin North Am* 1973;11:295-316
4. El-Zammar OA, Katzenstein AL. Pathological diagnosis of granulomatous lung disease: a review. *Histopathology* 2007;50:289-310
5. Colby TV, Specks U. Wegener's granulomatosis in the 1990s--a pulmonary pathologist's perspective. *Monogr Pathol* 1993;36:195-218
6. Mukhopadhyay S, Gal AA. Granulomatous lung disease: an approach to the differential diagnosis. *Arch Pathol Lab Med* 2010;134:667-690
7. Adams DO. The granulomatous inflammatory response. A review. *Am J Pathol* 1976;84:164-192
8. Hutton Klein JR, Tazelaar HD, Leslie KO, Colby TV. One hundred consecutive granulomas in a pulmonary pathology consultation practice. *Am J Surg Pathol* 2010;34:1456-1464
9. Mahdaviani SA, Mohajerani SA, Rezaei N, Casanova JL, Mansouri SD, Velayati AA. Pulmonary manifestations of chronic granulomatous disease. *Expert Rev Clin Immunol* 2013;9:153-160
10. Sergew A, Fernández Pérez ER. Current approach to diagnosis and management of pulmonary eosinophilic syndromes: eosinophilic pneumonias, eosinophilic granulomatosis with polyangiitis, and hypereosinophilic syndrome. *Semin Respir Crit Care Med* 2016;37:441-456
11. Low SE, Nicol A. Talc induced pulmonary granulomatosis. *J Clin Pathol* 2006;59:223
12. Lohrmann C, Uhl M, Kotter E, Burger D, Ghanem N, Langer M. Pulmonary manifestations of wegener granulomatosis: CT findings in 57 patients and a review of the literature. *Eur J Radiol* 2005;53:471-477
13. Jolly M, Molta C, Hoffman G. Wegener's granulomatosis: pitfalls in the management of pulmonary disease: a case of Wegener's granulomatosis with a hilar mass. *J Rheumatol* 2000;27:2511-2512
14. Stebbing J, Askin F, Fishman E, Stone J. Pulmonary manifestations of ulcerative colitis mimicking Wegener's granulomatosis. *J Rheumatol* 1999;26:1617-1621

15. Bargagli E, Prasse A. Sarcoidosis: a review for the internist. *Intern Emerg Med* 2018;13:325-331

16. Bonifazi M, Gasparini S, Alfieri V, Renzoni EA. Pulmonary sarcoidosis. *Semin Respir Crit Care Med* 2017;38:437-449

17. Rybicki BA, Maliarik MJ, Major M, Popovich J Jr, Iannuzzi MC. Epidemiology, demographics, and genetics of sarcoidosis. *Semin Respir Infect* 1998;13:166-173

18. Iannuzzi MC, Rybicki BA, Teirstein AS. Sarcoidosis. *N Engl J Med* 2007;357:2153-2165

19. Valeyre D, Bernaudin JF, Uzunhan Y, Kambouchner M, Brillet PY, Soussan M, et al. Clinical presentation of sarcoidosis and diagnostic work-up. *Semin Respir Crit Care Med* 2014;35:336-351

20. Grunewald J, Eklund A. Löfgren's syndrome: human leukocyte antigen strongly influences the disease course. *Am J Respir Crit Care Med* 2009;179:307-312

21. Karakaya B, Kaiser Y, van Moorsel CHM, Grunewald J. Löfgren's syndrome: diagnosis, management, and disease pathogenesis. *Semin Respir Crit Care Med* 2017;38:463-476

22. Agarwal S, Healey TT. Cardiothoracic complications of immune checkpoint inhibitor therapy: an imaging review. *J Comput Assist Tomogr* 2020;44:652-655

23. Ma Y, Gal A, Koss MN. The pathology of pulmonary sarcoidosis: update. *Semin Diagn Pathol* 2007;24:150-161

24. Criado E, Sánchez M, Ramírez J, Arguis P, de Caralt TM, Perea RJ, et al. Pulmonary sarcoidosis: typical and atypical manifestations at high-resolution CT with pathologic correlation. *Radiographics* 2010;30:1567-1586

25. Ganeshan D, Menias CO, Lubner MG, Pickhardt PJ, Sandrasegaran K, Bhalla S. Sarcoidosis from head to toe: what the radiologist needs to know. *Radiographics* 2018;38:1180-1200

26. Rubinstein I, Solomon A, Baum GL, Hiss Y. Pulmonary sarcoidosis presenting with unusual roentgenographic manifestations. *Eur J Respir Dis* 1985;67:335-340

27. Costabel U, Hunninghake GW. ATS/ERS/WASOG statement on sarcoidosis. Sarcoidosis Statement Committee. American Thoracic Society. European Respiratory Society. World Association for Sarcoidosis and Other Granulomatous Disorders. *Eur Respir J* 1999;14:735-737

28. Lynch JP 3rd, Ma YL, Koss MN, White ES. Pulmonary sarcoidosis. *Semin Respir Crit Care Med* 2007;28:53-74

29. Rosen Y, Moon S, Huang CT, Gourin A, Lyons HA. Granulomatous pulmonary angiitis in sarcoidosis. *Arch Pathol Lab Med* 1977;101:170-174

30. Churg A, Bilawich A, Wright JL. Pathology of chronic hypersensitivity pneumonitis what is it? What are the diagnostic criteria? Why do we care? *Arch Pathol Lab Med* 2018;142:109-119

31. Nishino M, Lee KS, Itoh H, Hatabu H. The spectrum of pulmonary sarcoidosis: variations of high-resolution CT findings and clues for specific diagnosis. *Eur J Radiol* 2010;73:66-73

32. Ramachandraiah V, Aronow W, Chandy D. Pulmonary

33. Teirstein AT, Morgenthau AS. "End-stage" pulmonary fibrosis in sarcoidosis. *Mt Sinai J Med* 2009;76:30-36

34. Cozzi D, Bargagli E, Calabrò AG, Torricelli E, Giannelli F, Cavigli E, et al. Atypical HRCT manifestations of pulmonary sarcoidosis. *Radiol Med* 2018;123:174-184

35. Nunes H, Uzunhan Y, Gille T, Lamberto C, Valeyre D, Brillet PY. Imaging of sarcoidosis of the airways and lung parenchyma and correlation with lung function. *Eur Respir J* 2012;40:750-765

36. Gera K, Panjabi C, Dash D, Shah A. Cavitary alveolar sarcoidosis complicated by an aspergilloma. *BMJ Case Rep* 2014;2014:bcr2014206280

37. Kantartzis SN, Dacic S, Strollo DC. AIRP best cases in radiologic-pathologic correlation: pulmonary sarcoidosis complicated by aspergilloma formation. *Radiographics* 2012;32:469-473

38. Israel HL, Lenchner GS, Atkinson GW. Sarcoidosis and aspergilloma. The role of surgery. *Chest* 1982;82:430-432

39. Liebow AA. The J. Burns Amberson lecture--pulmonary angiitis and granulomatosis. *Am Rev Respir* Dis 1973;108:1-18

40. Schiekofer S, Zirngibl C, Schneider JG. Necrotizing sarcoid granulomatosis (NSG): a diagnostic pitfall to watch out for! *J Clin Diagn Res* 2015;9:0J02

41. Giraudo C, Nannini N, Balestro E, Meneghin A, Lunardi F, Polverosi R, et al. Necrotizing sarcoid granulomatosis with an uncommon manifestation: clinicopathological features and review of literature. *Respir Care* 2014;59:e132-e136

42. Popper HH, Klemen H, Colby TV, Churg A. Necrotizing sarcoid granulomatosis--is it different from nodular sarcoidosis? *Pneumologie* 2003;57:268-271

43. Koss MN, Hochholzer L, Feigin DS, Garancis JC, Ward PA. Necrotizing sarcoid-like granulomatosis: clinical, pathologic, and immunopathologic findings. *Hum Pathol* 1980;11:510-519

44. Yeboah J, Afkhami M, Lee C, Sharma OP. Necrotizing sarcoid granulomatosis. *Curr Opin Pulm Med* 2012;18:493-498

45. Ma Y, Gal A, Koss M. Reprint of: the pathology of pulmonary sarcoidosis: update. *Semin Diagn Pathol* 2018;35:324-333

46. Karpathiou G, Batistatou A, Boglou P, Stefanou D, Froudarakis ME. Necrotizing sarcoid granulomatosis: a distinctive form of pulmonary granulomatous disease. *Clin Respir J* 2018;12:1313-1319

47. Rosen Y. Four decades of necrotizing sarcoid granulomatosis: what do we know now? *Arch Pathol Lab Med* 2015;139:252-262

48. Shibata T, Takahashi K, Uchida M, Yamasaki F, Kawashima M, Sueoka-Aragane N. Necrotizing sarcoid granulomatosis with natural resolution after a surgical lung biopsy. *Intern Med* 2018;57:1625-1629

49. Fisher MR, Christ ML, Bernstein JR. Necrotizing sarcoid-like granulomatosis: radiologic-pathologic correlation. *J Can Assoc Radiol* 1984;35:313-315

50. Quaden C, Tillie-Leblond I, Delobbe A, Delaunois L, Verstraeten A, Demedts M, et al. Necrotising sarcoid granulomatosis: clinical, functional, endoscopical and radiographical evaluations. *Eur Respir J* 2005;26:778-785

51. Myers JL, Kurtin PJ, Katzenstein AL, Tazelaar HD, Colby TV, Strickler JG, et al. Lymphomatoid granulomatosis. Evidence of immunophenotypic diversity and relationship to Epstein-Barr virus infection. *Am J Surg Pathol* 1995;19:1300-1312

52. Katzenstein AL, Doxtader E, Narendra S. Lymphomatoid granulomatosis: insights gained over 4 decades. *Am J Surg Pathol* 2010;34:e35-e48

53. Katzenstein AL, Carrington CB, Liebow AA. Lymphomatoid granulomatosis: a clinicopathologic study of 152 cases. *Cancer* 1979;43:360-373

54. Guinee D Jr, Jaffe E, Kingma D, Fishback N, Wallberg K, Krishnan J, et al. Pulmonary lymphomatoid granulomatosis. Evidence for a proliferation of Epstein-Barr virus infected B-lymphocytes with a prominent T-cell component and vasculitis. *Am J Surg Pathol* 1994;18:753-764

55. Sordillo PP, Epremian B, Koziner B, Lacher M, Lieberman P. Lymphomatoid granulomatosis: an analysis of clinical and immunologic characteristics. *Cancer* 1982;49:2070-2076

56. Leonard JP, Martin P, Roboz GJ. Practical implications of the 2016 revision of the World Health Organization classification of lymphoid and myeloid neoplasms and acute leukemia. *J Clin Oncol* 2017;35:2708-2715

57. Sirajuddin A, Raparia K, Lewis VA, Franks TJ, Dhand S, Galvin JR, et al. Primary pulmonary lymphoid lesions: radiologic and pathologic findings. *Radiographics* 2016;36:53-70

58. Lee JS, Tuder R, Lynch DA. Lymphomatoid granulomatosis: radiologic features and pathologic correlations. *AJR Am J Roentgenol* 2000;175:1335-1339

59. Benamore RE, Weisbrod GL, Hwang DM, Bailey DJ, Pierre AF, Lazar NM, et al. Reversed halo sign in lymphomatoid granulomatosis. *Br J Radiol* 2007;80:e162-e166

60. Marchiori E, Zanetti G, Hochhegger B, Irion KL, Carvalho AC, Godoy MC. Reversed halo sign on computed tomography: state-of-the-art review. *Lung* 2012;190:389-394

61. Chung JH, Wu CC, Gilman MD, Palmer EL, Hasserjian RP, Shepard JA. Lymphomatoid granulomatosis: CT and FDG-PET findings. *Korean J Radiol* 2011;12:671-678

62. Park JH, Levinson AI. Granulomatous-lymphocytic interstitial lung disease (GLILD) in common variable immunodeficiency (CVID). *Clin Immunol* 2010;134:97-103

63. Cunningham-Rundles C. Common variable immune deficiency: dissection of the variable. *Immunol Rev* 2019;287:145-161

64. Mooney D, Edgar D, Einarsson G, Downey D, Elborn S, Tunney M. Chronic lung disease in common variable immune deficiency (CVID): a pathophysiological role for microbial and non-B cell immune factors. *Crit Rev Microbiol* 2017;43:508-519

65. Gupta S, Pattanaik D, Krishnaswamy G. Common variable immune deficiency and associated complications. *Chest* 2019;156:579-593

66. Abbott JK, Gelfand EW. Common variable immunodeficiency: diagnosis, management, and treatment. *Immunol Allergy Clin North Am* 2015;35:637-658

67. Kiaee F, Azizi G, Rafiemanesh H, Zainaldain H, Sadaat Rizvi F, Alizadeh M, et al. Malignancy in common variable immunodeficiency: a systematic review and meta-analysis. *Expert Rev Clin Immunol* 2019;15:1105-1113

68. Maarschalk-Ellerbroek LJ, de Jong PA, van Montfrans JM, Lammers JW, Bloem AC, Hoepelman AI, et al. CT screening for pulmonary pathology in common variable immunodeficiency disorders and the correlation with clinical and immunological parameters. *J Clin Immunol* 2014;34:642-654

69. van Zeggeren L, van de Ven AA, Terheggen-Lagro SW, Mets OM, Beek FJ, van Montfrans JM, et al. High-resolution computed tomography and pulmonary function in children with common variable immunodeficiency. *Eur Respir J* 2011;38:1437-1443

70. Gharagozlou M, Ebrahimi FA, Farhoudi A, Aghamohammadi A, Bemanian MH, Chavoshzadeh Z, et al. Pulmonary complications in primary hypogammaglobulinemia: a survey by high resolution CT scan. *Monaldi Arch Chest Dis* 2006;65:69-74

71. Bang TJ, Richards JC, Olson AL, Groshong SD, Gelfand EW, Lynch DA. Pulmonary manifestations of common variable immunodeficiency. *J Thorac Imaging* 2018;33:377-383

72. Park JE, Beal I, Dilworth JP, Tormey V, Haddock J. The HRCT appearances of granulomatous pulmonary disease in common variable immune deficiency. *Eur J Radiol* 2005;54:359-364

73. Maglione PJ, Overbey JR, Radigan L, Bagiella E, Cunningham-Rundles C. Pulmonary radiologic findings in common variable immunodeficiency: clinical and immunological correlations. *Ann Allergy Asthma Immunol* 2014;113:452-459

74. Tashtoush B, Memarpour R, Ramirez J, Bejarano P, Mehta J. Granulomatous-lymphocytic interstitial lung disease as the first manifestation of common variable immunodeficiency. *Clin Respir J* 2018;12:337-343

75. Larsen BT, Smith ML, Tazelaar HD, Yi ES, Ryu JH, Churg A. GLILD revisited: pulmonary pathology of common variable and selective IgA immunodeficiency. *Am J Surg Pathol* 2020;44:1073-1081

76. Hurst JR, Verma N, Lowe D, Baxendale HE, Jolles S, Kelleher P, et al. British Lung Foundation/United Kingdom Primary Immunodeficiency Network consensus statement on the definition, diagnosis, and management of granulomatous-lymphocytic interstitial lung disease in common variable immunodeficiency disorders. *J Allergy Clin Immunol Pract* 2017;5:938-945

77. Prather AD, Smith TR, Poletto DM, Tavora F, Chung JH, Nallamshetty L, et al. Aspiration-related lung diseases. *J Thorac Imaging* 2014;29:304-309

78. Lee AS, Ryu JH. Aspiration pneumonia and related syndromes. *Mayo Clin Proc* 2018;93:752-762

79. Scheeren B, Gomes E, Alves G, Marchiori E, Hochhegger B. Chest CT findings in patients with dysphagia and aspiration: a systematic review. *J Bras Pneumol* 2017;43:313-318

80. Hu X, Lee JS, Pianosi PT, Ryu JH. Aspiration-related pulmonary syndromes. *Chest* 2015;147:815-823

81. Franquet T, Giménez A, Rosón N, Torrubia S, Sabaté JM, Pérez C. Aspiration diseases: findings, pitfalls, and differential diagnosis. *Radiographics* 2000;20:673-685

82. Lee AS, Lee JS, He Z, Ryu JH. Reflux-aspiration in chronic lung disease. *Ann Am Thorac Soc* 2020;17:155-164

83. Marom EM, McAdams HP, Sporn TA, Goodman PC. Lentil aspiration pneumonia: radiographic and CT findings. *J Comput Assist Tomogr* 1998;22:598-600

84. Marom EM, McAdams HP, Erasmus JJ, Goodman PC. The many faces of pulmonary aspiration. *AJR Am J Roentgenol* 1999;172:121-128

85. Paré JP, Cote G, Fraser RS. Long-term follow-up of drug abusers with intravenous talcosis. *Am Rev Respir Dis* 1989;139:233-241

86. Chong S, Lee KS, Chung MJ, Han J, Kwon OJ, Kim TS. Pneumoconiosis: comparison of imaging and pathologic findings. *Radiographics* 2006;26:59-77

87. Escuissato DL, Ferreira RG, Barros JA, Marchiori E. Pulmonary talcosis caused by intravenous methadone injection. *J Bras Pneumol* 2017;43:154-155

88. van Huisstede A, Noordhoek Hegt V, Otte-Holler I, Looijen-Salamon M, Rudolphus A. Talcosis due to abundant use of cosmetic talcum powder. *Eur Respir Rev* 2010;19:165-168

89. Ward S, Heyneman LE, Reittner P, Kazerooni EA, Godwin JD, Müller NL. Talcosis associated with IV abuse of oral medications: CT findings. *AJR Am J Roentgenol* 2000;174:789-793

90. Verlynde G, Agneessens E, Dargent JL. Pulmonary talcosis due to daily inhalation of talc powder. *J Belg Soc Radiol* 2018;102:12

91. Mark GJ, Monroe CB, Kazemi H. Mixed pneumoconiosis: silicosis, asbestosis, talcosis, and berylliosis. *Chest* 1979;75:726-728

92. Kleinfeld M, Messite J, Kooyman O, Shapiro J. Pulmonary ventilatory function in talcosis of lung. *Dis Chest* 1964;46:592-598

93. Nguyen VT, Chan ES, Chou SH, Godwin JD, Fligner CL, Schmidt RA, et al. Pulmonary effects of i.v. injection of crushed oral tablets: "excipient lung disease". *AJR Am J Roentgenol* 2014;203:W506-W515

94. Siddiqui MF, Saleem S, Badireddi S. Pulmonary talcosis with intravenous drug abuse. *Respir Care* 2013;58:e126-e128

95. Griffith CC, Raval JS, Nichols L. Intravascular talcosis due to intravenous drug use is an underrecognized cause of pulmonary hypertension. *Pulm Med* 2012;2012:617531

96. Chang CJ, Tu YK, Chen PC, Yang HY. Occupational exposure to talc increases the risk of lung cancer: a meta-analysis of occupational cohort studies. *Can Respir J* 2017;2017:1270608

97. Wergeland E, Andersen A, Baerheim A. Morbidity and mortality in talc-exposed workers. *Am J Ind Med* 1990;17:505-513

98. Restrepo CS, Carrillo JA, Martínez S, Ojeda P, Rivera AL, Hatta A. Pulmonary complications from cocaine and cocaine-based substances: imaging manifestations. *Radiographics* 2007;27:941-956

99. Ergönül AG, Çakan A, Çağirici U, Nart D. Talc granulomatosis with multiple parenchymal and pleural nodules. *Eur J Cardiothorac Surg* 2013;44:e308

100. Marchiori E, Lourenço S, Gasparetto TD, Zanetti G, Mano CM, Nobre LF. Pulmonary talcosis: imaging findings. *Lung* 2010;188:165-171

101. Pereira Faria H, de Souza Veiga A, Coutinho Teixeira L, de Paula Alves Bezerra OM, Scalia Carneiro AP, Ferreira CS, et al. Talcosis in soapstone artisans: high-resolution CT findings in 12 patients. *Clin Radiol* 2014;69:e136-e139

102. Pomeranz R, Brodkin HA. Berylliosis and silicosis. *J Int Coll Surg* 1951;15:633-638

103. Machle W. Berylliosis; observations and report of clinical study of 70 cases of chronic disease. *J Lab Clin Med* 1948;33:1613

104. Martínez González C, Casan Clara P, Prieto Fernández A, Alonso Arias R. Berylliosis: a granulomatosis to remind us of the importance of occupational history. *Arch Bronconeumol* 2020;56:470-471

105. Schubert J. Beryllium and berylliosis. *Sci Am* 1958;199:27-33

106. Balmes JR, Abraham JL, Dweik RA, Fireman E, Fontenot AP, Maier LA, et al. An official American Thoracic Society statement: diagnosis and management of beryllium sensitivity and chronic beryllium disease. *Am J Respir Crit Care Med* 2014;190:e34-e59

107. Maier LA. Clinical approach to chronic beryllium disease and other nonpneumoconiotic interstitial lung diseases. *J Thorac Imaging* 2002;17:273-284

108. Sprince NL, Kanarek DJ, Weber AL, Chamberlin RI, Kazemi H. Reversible respiratory disease in beryllium workers. *Am Rev Respir Dis* 1978;117:1011-1017

109. Sirajuddin A, Kanne JP. Occupational lung disease. *J Thorac Imaging* 2009;24:310-320

110. Williams WJ. Beryllium workers--sarcoidosis or chronic beryllium disease. *Sarcoidosis* 1989;6 Suppl 1:34-35

111. Newman LS, Kreiss K. Nonoccupational beryllium disease masquerading as sarcoidosis: identification by blood lymphocyte proliferative response to beryllium. *Am Rev Respir Dis* 1992;145:1212-1214

112. Mayer AS, Hamzeh N, Maier LA. Sarcoidosis and chronic beryllium disease: similarities and differences. *Semin Respir Crit Care Med* 2014;35:316-329

113. Weissman DN. Role of chest computed tomography in prevention of occupational respiratory disease: review of recent literature. *Semin Respir Crit Care Med* 2015;36:433-448

114. Flors L, Domingo ML, Leiva-Salinas C, Mazón M, Roselló-Sastre E, Vilar J. Uncommon occupational lung diseases: high-resolution CT findings. *AJR Am J Roentgenol* 2010;194:W20-W26

115. Sharma N, Patel J, Mohammed TL. Chronic beryllium disease: computed tomographic findings. *J Comput Assist Tomogr* 2010;34:945-948

116. Champlin J, Edwards R, Pipavath S. Imaging of occupational lung disease. *Radiol Clin North Am* 2016;54:1077-1096

117. Spagnolo P, Rossi G, Cavazza A, Bonifazi M, Paladini I, Bonella F, et al. Hypersensitivity pneumonitis: a comprehensive review. *J Investig Allergol Clin Immunol* 2015;25:237-250; quiz follow 250

118. Sharma OP, Fujimura N. Hypersensitivity pneumonitis: a noninfectious granulomatosis. *Semin Respir Infect* 1995;10:96-106

119. Morisset J, Johannson KA, Jones KD, Wolters PJ, Collard HR, Walsh SLF, et al. Identification of diagnostic criteria for chronic hypersensitivity pneumonitis. An International Modified Delphi Survey. *Am J Respir Crit Care Med* 2018;197:1036-1044

120. Lacasse Y, Selman M, Costabel U, Dalphin JC, Morell F, Erkinjuntti-Pekkanen R, et al. Classification of hypersensitivity pneumonitis: a hypothesis. *Int Arch Allergy Immunol* 2009;149:161-166

121. Miller R, Allen TC, Barrios RJ, Beasley MB, Burke L, Cagle PT, et al. Hypersensitivity pneumonitis a perspective from members of the pulmonary pathology society. *Arch Pathol Lab Med* 2018;142:120-126

122. Castonguay MC, Ryu JH, Yi ES, Tazelaar HD. Granulomas and giant cells in hypersensitivity pneumonitis. *Hum Pathol* 2015;46:607-613

123. Magee AL, Montner SM, Husain A, Adegunsoye A, Vij R, Chung JH. Imaging of hypersensitivity pneumonitis. *Radiol Clin North Am* 2016;54:1033-1046

124. Franquet T, Hansell DM, Senbanjo T, Remy-Jardin M, Müller NL. Lung cysts in subacute hypersensitivity pneumonitis. *J Comput Assist Tomogr* 2003;27:475-478

125. Selman M, Pardo A, King TE Jr. Hypersensitivity pneumonitis: insights in diagnosis and pathobiology. *Am J Respir Crit Care Med* 2012;186:314-324

126. Silva CI, Müller NL, Lynch DA, Curran-Everett D, Brown KK, Lee KS, et al. Chronic hypersensitivity pneumonitis: differentiation from idiopathic pulmonary fibrosis and nonspecific interstitial pneumonia by using thin-section CT. *Radiology* 2008;246:288-297

127. Dias OM, Baldi BG, Pennati F, Aliverti A, Chate RC, Sawamura MVY, et al. Computed tomography in hypersensitivity pneumonitis: main findings, differential diagnosis and pitfalls. *Expert Rev Respir Med* 2018;12:5-13

128. Morell F, Villar A, Ojanguren I, Muñoz X, Cruz MJ, Sansano I, et al. Hypersensitivity Pneumonitis and (idiopathic) pulmonary fibrosis due to feather duvets and pillows. *Arch Bronconeumol* 2021;57:87-93

129. Morell F, Villar A, Montero MÁ, Muñoz X, Colby TV, Pipvath S, et al. Chronic hypersensitivity pneumonitis in patients diagnosed with idiopathic pulmonary fibrosis: a prospective case-cohort study. *Lancet Respir Med* 2013;1:685-694

130. Hoffman GS, Kerr GS, Leavitt RY, Hallahan CW, Lebovics RS, Travis WD, et al. Wegener granulomatosis: an analysis of 158 patients. *Ann Intern Med* 1992;116:488-498

131. Grygiel-Górniak B, Limphaibool N, Perkowska K, Puszczewicz M. Clinical manifestations of granulomatosis with polyangiitis: key considerations and major features. *Postgrad Med* 2018;130:581-596

132. Martinez F, Chung JH, Digumarthy SR, Kanne JP, Abbott GF, Shepard JA, et al. Common and uncommon manifestations of Wegener granulomatosis at chest CT: radiologic-pathologic correlation. *Radiographics* 2012;32:51-69

133. Travis WD. Common and uncommon manifestations of wegener's granulomatosis. *Cardiovasc Pathol* 1994;3:217-225

134. Travis WD. Pathology of pulmonary vasculitis. *Semin Respir Crit Care Med* 2004;25:475-482

135. Uner AH, Rozum-Slota B, Katzenstein AL. Bronchiolitis obliterans-organizing pneumonia (BOOP)-like variant of Wegener's granulomatosis. A clinicopathologic study of 16 cases. *Am J Surg Pathol* 1996;20:794-801

136. Castañer E, Alguersuari A, Gallardo X, Andreu M, Pallardó Y, Mata JM, et al. When to suspect pulmonary vasculitis: radiologic and clinical clues. *Radiographics* 2010;30:33-53

137. Feragalli B, Mantini C, Sperandeo M, Galluzzo M, Belcaro G, Tartaro A, et al. The lung in systemic vasculitis: radiological patterns and differential diagnosis. *Br J Radiol* 2016;89:20150992

138. Lee KS, Kim TS, Fujimoto K, Moriya H, Watanabe H, Tateishi U, et al. Thoracic manifestation of Wegener's granulomatosis: CT findings in 30 patients. *Eur Radiol* 2003;13:43-51

139. Sheth JS, Belperio JA, Fishbein MC, Kazerooni EA, Lagstein A, Murray S, et al. Utility of transbronchial vs surgical lung biopsy in the diagnosis of suspected fibrotic interstitial lung disease. *Chest* 2017;151:389-399

140. Castañer E, Alguersuari A, Andreu M, Gallardo X, Spinu C, Mata JM. Imaging findings in pulmonary vasculitis. *Semin Ultrasound CT MR* 2012;33:567-579

141. Kuhlman JE, Hruban RH, Fishman EK. Wegener granulomatosis: CT features of parenchymal lung disease. *J Comput Assist Tomogr* 1991;15:948-952

142. Guneyli S, Ceylan N, Bayraktaroglu S, Gucenmez S, Aksu K, Kocacelebi K, et al. Imaging findings of pulmonary granulomatosis with polyangiitis (Wegener's granulomatosis): lesions invading the pulmonary fissure, pleura or diaphragm mimicking malignancy. *Wien Klin Wochenschr* 2016;128:809-815

143. Ananthakrishnan L, Sharma N, Kanne JP. Wegener's granulomatosis in the chest: high-resolution CT findings. *AJR Am J Roentgenol* 2009;192:676-682

144. Aberle DR, Gamsu G, Lynch D. Thoracic manifestations of Wegener granulomatosis: diagnosis and course. *Radiology*

1990;174:703-709

145. Papiris SA, Manoussakis MN, Drosos AA, Kontogiannis D, Constantopoulos SH, Moutsopoulos HM. Imaging of thoracic Wegener's granulomatosis: the computed tomographic appearance. *Am J Med* 1992;93:529-536

146. Cordier JF, Cottin V. Alveolar hemorrhage in vasculitis: primary and secondary. *Semin Respir Crit Care Med* 2011;32:310-321

147. Cordier JF. Organizing pneumonia: cryptogenic and disease associated. *Semin Respir Crit Care Med* 2003;24:595-606

148. Cordier JF, Cottin V, Lazor R, Thivolet-Béjui F. Many faces of bronchiolitis and organizing pneumonia. *Semin Respir Crit Care Med* 2016;37:421-440

149. Jennette JC, Falk RJ, Bacon PA, Basu N, Cid MC, Ferrario F, et al. 2012 revised international chapel hill consensus conference nomenclature of vasculitides. *Arthritis Rheum* 2013;65:1-11

150. Masi AT, Hunder GG, Lie JT, Michel BA, Bloch DA, Arend WP, et al. The American College of Rheumatology 1990 criteria for the classification of Churg-Strauss syndrome (allergic granulomatosis and angiitis). *Arthritis Rheum* 1990;33:1094-1100

151. Guillevin L, Pagnoux C, Mouthon L. Churg-strauss syndrome. *Semin Respir Crit Care Med* 2004;25:535-545

152. Neumann T, Manger B, Schmid M, Kroegel C, Hansch A, Kaiser WA, et al. Cardiac involvement in Churg-Strauss syndrome: impact of endomyocarditis. *Medicine (Baltimore)* 2009;88:236-243

153. Keogh KA, Specks U. Churg-Strauss syndrome. *Semin Respir Crit Care Med* 2006;27:148-157

154. Cottin V, Bel E, Bottero P, Dalhoff K, Humbert M, Lazor R, et al. Respiratory manifestations of eosinophilic granulomatosis with polyangiitis (Churg-Strauss). *Eur Respir J* 2016;48:1429-1441

155. Greco A, Rizzo MI, De Virgilio A, Gallo A, Fusconi M, Ruoppolo G, et al. Churg-Strauss syndrome. *Autoimmun Rev* 2015;14:341-348

156. Scapa JV, Fishbein GA, Wallace WD, Fishbein MC. Diffuse alveolar hemorrhage and pulmonary vasculitides: histopathologic findings. *Semin Respir Crit Care Med* 2018;39:425-433

157. Choi YH, Im JG, Han BK, Kim JH, Lee KY, Myoung NH. Thoracic manifestation of Churg-Strauss syndrome: radiologic and clinical findings. *Chest* 2000;117:117-124

158. Worthy SA, Müller NL, Hansell DM, Flower CD. Churg-Strauss syndrome: the spectrum of pulmonary CT findings in 17 patients. *AJR Am J Roentgenol* 1998;170:297-300

159. Silva CI, Müller NL, Fujimoto K, Johkoh T, Ajzen SA, Churg A. Churg-Strauss syndrome: high resolution CT and pathologic findings. *J Thorac Imaging* 2005;20:74-80

160. Szczeklik W, Sokołowska B, Mastalerz L, Grzanka P, Górka J, Pacułt K, et al. Pulmonary findings in Churg-Strauss syndrome in chest X-rays and high resolution computed tomography at the time of initial diagnosis. *Clin Rheumatol* 2010;29:1127-1134

161. Bang S, Kim Y, Jang K, Paik SS, Shin SJ. Clinicopathologic features of rheumatoid nodules: a retrospective analysis. *Clin Rheumatol* 2019;38:3041-3048

162. Jolles H, Moseley PL, Peterson MW. Nodular pulmonary opacities in patients with rheumatoid arthritis. A diagnostic dilemma. *Chest* 1989;96:1022-1025

163. Hurd ER. Extraarticular manifestations of rheumatoid arthritis. *Semin Arthritis Rheum* 1979;8:151-176

164. Brown KK. Rheumatoid lung disease. *Proceedings of the American Thoracic Society* 2007;4:443-448

165. Franquet T. High-resolution CT of lung disease related to collagen vascular disease. *Radiol Clin North Am* 2001;39:1171-1187

166. Portner MM, Gracie WA Jr. Rheumatoid lung disease with cavitary nodules, pneumothorax and eosinophilia. *N Engl J Med* 1966;275:697-700

167. Chaudhry AA, Gul M, Chaudhry AA, Moore W. Case 238: spontaneous pneumothorax secondary to intrapulmonary necrobiotic rheumatoid nodule. *Radiology* 2017;282:602-608

168. Yousem SA, Colby TV, Carrington CB. Lung biopsy in rheumatoid arthritis. *Am Rev Respir Dis* 1985;131:770-777

169. Highton J, Hung N, Hessian P, Wilsher M. Pulmonary rheumatoid nodules demonstrating features usually associated with rheumatoid synovial membrane. *Rheumatology (Oxford)* 2007;46:811-814

170. Koslow M, Young JR, Yi ES, Baqir M, Decker PA, Johnson GB, et al. Rheumatoid pulmonary nodules: clinical and imaging features compared with malignancy. *Eur Radiol* 2019;29:1684-1692